

UNIVERSIDADE FEDERAL DO PARANÁ

AURORA MACHADO GARCIA

MICROMORFOLOGIA DE FÁCIES DEFORMADAS DO GRUPO ITARARÉ E
FORMAÇÃO AQUIDAUANA, PALEOZOICO SUPERIOR DA BACIA DO PARANÁ

CURITIBA

2020

UNIVERSIDADE FEDERAL DO PARANÁ

AURORA MACHADO GARCIA

MICROMORFOLOGIA DE FÁCIES DEFORMADAS DO GRUPO ITARARÉ E
FORMAÇÃO AQUIDAUANA, PALEOZOICO SUPERIOR DA BACIA DO PARANÁ

Dissertação apresentada como requisito parcial à
obtenção do grau de Mestre em Geologia junto ao
Programa de Pós-Graduação em Geologia. Área
de Concentração em Geologia Exploratória, Setor
de Ciências da Terra, Universidade Federal do
Paraná.

Orientadora: Profa. Dra. Bárbara Trzaskos

Coorientador: Prof. Dr. Fernando Farias Vesely

CURITIBA

2020

Catálogo na Fonte: Sistema de Bibliotecas, UFPR
Biblioteca de Ciência e Tecnologia

G216m

Garcia, Aurora Machado

Micromorfologia de fácies deformadas do Grupo Itararé e Formação Aquidauana, Paleozoico Superior da Bacia do Paraná [recurso eletrônico] / Aurora Machado Garcia. – Curitiba, 2020.

Dissertação - Universidade Federal do Paraná, Setor de Ciências da Terra, Programa de Pós-Graduação em Geologia, 2020.

Orientador: Bárbara Trzaskos – Coorientador: Fernando Farias Vesely

1. Movimentos de massa. 2. Petrografia. 3. Glaciologia. 4. Tectônica (Geologia). 5. Geomorfologia. I. Universidade Federal do Paraná. II. Trzaskos, Bárbara. III. Vesely, Fernando Farias. IV. Título.

CDD: 624.1513

Bibliotecário: Elias Barbosa da Silva CRB-9/1894

TERMO DE APROVAÇÃO

Os membros da Banca Examinadora designada pelo Colegiado do Programa de Pós-Graduação em GEOLOGIA da Universidade Federal do Paraná foram convocados para realizar a arguição da dissertação de Mestrado de **AURORA MACHADO GARCIA** intitulada: **MICROMORFOLOGIA DE FÁCIES DEFORMADAS DO GRUPO ITARARÉ E FORMAÇÃO AQUIDAUANA, PALEOZOICO SUPERIOR DA BACIA DO PARANÁ**, sob orientação da Profa. Dra. BÁRBARA TRZASKOS, que após terem inquirido a aluna e realizada a avaliação do trabalho, são de parecer pela sua APROVAÇÃO no rito de defesa.

A outorga do título de mestre está sujeita à homologação pelo colegiado, ao atendimento de todas as indicações e correções solicitadas pela banca e ao pleno atendimento das demandas regimentais do Programa de Pós-Graduação.

CURITIBA, 27 de Maio de 2020.

Assinatura Eletrônica

28/05/2020 10:27:45.0

BÁRBARA TRZASKOS

Presidente da Banca Examinadora (UNIVERSIDADE FEDERAL DO PARANÁ)

Assinatura Eletrônica

28/05/2020 10:32:23.0

CARLOS CONFORTI FERREIRA GUEDES

Avaliador Interno (UNIVERSIDADE FEDERAL DO PARANÁ)

Assinatura Eletrônica

28/05/2020 17:05:42.0

CLAUDIO LIMEIRA MELLO

Avaliador Externo (UNIVERSIDADE FEDERAL DO RIO DE JANEIRO)

AGRADECIMENTOS

Gostaria de agradecer primeiramente ao Programa de Pós-Graduação em Geologia da Universidade Federal do Paraná pela oportunidade de realização deste trabalho. À CAPES pela concessão da bolsa de mestrado e ao projeto Caruaçu da Petrobras pelo financiamento de campos e confecção de lâminas petrográficas.

Ao LABAP não só pela infraestrutura fornecida, mas pelo ambiente propício ao desenvolvimento da pesquisa, por todas as amizades que se iniciaram e ciência que foi discutida. Renata, Fábio, Lara, Thammy, Leonardo, Eduardo, Brunos, Mérolyn, Deise, Hugo e Nicole, foi uma honra dividir o laboratório com vocês.

Aos meus orientadores, Profa. Dra. Bárbara Trzaskos e Prof. Dr. Fernando Farias Vesely, cujas discussões em campo, laboratório e, recentemente, chamadas de vídeo foram essenciais para o desenvolvimento conjunto, tanto pessoal quanto acadêmico. Agradeço pelo apoio, confiança, aprendizado e até mesmo pelos eventuais puxões de orelha.

Aos membros da banca, Prof. Dr. Carlos Conforti Ferreira Guedes e Prof. Dr. Claudio Limeira Mello pelos valiosos e detalhados comentários e sugestões que sem dúvidas contribuíram em muito para o aprimoramento da pesquisa.

Agradeço ao Prof. PhD John Isbell, da University of Wisconsin-Milwaukee pelo campo para a Fm. Aquidauana que transformou completamente esta pesquisa e pelas discussões geológicas em inglês.

Ao PhD Emrys Phillips e ao Serviço Geológico Britânico que gentilmente me receberam na Escócia durante um período curto, porém de imenso aprendizado.

Ao Prof. Dr. Leonardo Lagoeiro, pelo empréstimo do scanner de alta resolução, primordial para a confecção desta pesquisa.

Àqueles muitos que me acompanharam em campo, Lucas, Eduardo, Leonardo, Lara, Thammy, Deise e Bruno, agradeço pela paciência de encarar longas caminhadas ao longo do trilho do trem, geralmente sob chuva.

Agradeço ainda a todos os meus amigos, de dentro ou fora da Geologia, que me apoiaram e incentivaram sempre nesta profissão que muitas vezes implica em longos períodos de ausência. Em especial, ao Lucas. Meu amigo desde o primeiro dia da graduação e hoje meu companheiro de vida. Agradeço por todo cuidado, estímulo e carinho, foi muito mais leve passar por tudo isso com você.

A todos aqueles que compõem e lutam pelas Universidades públicas brasileiras,

gratuitas e de qualidade.

Aos meus pais, não tenho palavras para expressar a felicidade que tenho em ser sua filha. Por tudo que vocês já fizeram e continuam fazendo por mim, sempre colocando meus estudos como prioridade. A distância nunca foi fácil, mas ela nunca diminuiu o amor e admiração que tenho por vocês. Este mestrado também é mérito de vocês.

A todos, muitíssimo obrigada.

RESUMO

O Grupo Itararé e a Formação Aquidauana, correlatos temporalmente, representam a *Late Paleozoic Ice Age* (LPIA) na Bacia do Paraná. Estas rochas sedimentares fornecem um registro glacial extenso, que contém intervalos deformados, interpretados como glacioteconitos, com feições incluindo dobras, cavalgamentos e zonas de cisalhamento sub-horizontais, que podem ser produzidas tanto sub- quanto pró glacialmente. Adicionalmente, ambas as unidades possuem uma significativa ocorrência de depósitos de transporte em massa, que são caracterizados principalmente como diamictitos lamosos com grandes blocos ressedimentados de arenitos e lamitos no Grupo Itararé e como diamictitos arenosos pobre em clastos na Formação Aquidauana. Estes depósitos possuem estruturas relacionadas à cisalhamento, distensão e compressão. Poucos estudos abordaram estruturas em microescala relacionadas à deformação de sedimentos em movimentos de massa e em depósitos glacioteconizados do Paleozoico ou mesmo períodos mais antigos, que podem ser obliteradas por eventos diagenéticos subsequentes. Este trabalho tem como objetivo adereçar este problema e correlacionar a gama de microestruturas presentes em lâmina petrográfica aos diferentes contextos deposicionais interpretados com base na descrição macroscópica de fácies sedimentares. Os resultados são utilizados para avaliar criticamente a aplicabilidade da micromorfologia na distinção de paleoambientes no registro glacial Pré-Pleistocênico e como estas estruturas podem ser modificadas com o tempo em resposta à litificação e diagênese. O estudo une dados de campo com análise micromorfológica e microestrutural detalhada de 40 seções delgadas do Grupo Itararé e Formação Aquidauana. Amostras foram coletadas de diferentes litotipos de diferentes contextos, incluindo diamictitos, arenitos e lamitos de transportes de massa e glacioteconitos sub- e pró-glaciais. As microestruturas presentes incluem *plasmic fabrics* uniaxiais, estruturas rotacionais, micro zonas de cisalhamento, clastos cisalhados, falhas, dobras, “*boudins*” e intraclastos. Porém, algumas fácies bem selecionadas, que contém pouca ou nenhuma matriz, também possuem feições tipicamente associadas com compactação e diagênese, como esmagamento de grãos, redução da porosidade primária, contatos suturados e estilólitos. Resultados mostram que sedimentos de diferentes contextos deposicionais podem conter assembleias similares de microestruturas. Isto sugere que apenas microestruturas não podem caracterizar por completo o contexto deposicional em sequências mais antigas. Além disso, a diagênese exerce um papel importante na preservação de estruturas sedimentares primárias e de deformação em estado inconsolidado, podendo levar à sobreposição destas estruturas caso a rocha tenha conteúdo baixo de matriz.

PALAVRAS CHAVE: GLACIOTECTONITO, MOVIMENTO DE MASSA, MICROMORFOLOGIA

ABSTRACT

The Itararé Group and time equivalent Aquidauana Formation represent the Late Paleozoic Ice Age in the Paraná Basin. These sedimentary rocks provide an extensive glacial record which contains deformed intervals interpreted as glacioteconites, with features such as folds, thrusts and subhorizontal shear zones, which could be produced sub- or proglacially. Additionally, both units have a significant occurrence of mass-transport deposits (MTDs), which are characterized mainly as muddy diamictites with major blocks of ressedimented arenites and mudstones in the Itararé Group and as mostly sandy diamictites clast-poor in the Aquidauana Formation. Those deposits also display structures related to shearing, distension and compression. Few studies have approached microscale deformation related to soft-sediment deformation, in mass transport deposits and glacially-related deposits from the Paleozoic or even older periods, which can be obliterated by subsequent diagenetic events. This study aims to address this issue and correlate the range of microstructures present in thin section to different depositional settings interpreted on the basis on macroscale sedimentary facies analysis. The results are used to critically evaluate the applicability of micromorphology in distinguishing paleoenvironments in the pre-Pleistocene glacial record and how those structures can be modified over time in response to lithification and diagenesis. The study combines field data with detailed micromorphological and microstructural analysis of 40 thin sections from the Itararé Group and the Aquidauana Formation. Samples were collected from a range of lithotypes from different depositional settings including: diamictites, sandstones and mudstones from, mass transport, subglacial overriding and ice-marginal glacioteconism. The microstructures present include unistrial plasmic fabrics, glacioteconic laminations, rotational structures (turbates), microshear zones, sheared clasts, faults, folds, boudins and intraclasts. However, in some well-sorted facies, which contain very little or no matrix, also contain features typically associated with compaction and diagenesis, such as grain crushing, reduction of primary porosity, sutured grain contacts and stylolites. Results show that sediments from a range of different depositional facies may contain a similar assemblage of microstructures. This suggests that microstructures on their own cannot fully characterize the deformational setting in older sequences. Furthermore, diagenesis plays a major role when it comes to the preservation of primary sedimentary and soft-sediment deformation features and can lead to the overprinting of these structures if the rock has a low content of matrix.

KEY-WORDS: GLACIOTECTONITE, MASS TRANSPORT DEPOSIT, MICROMORPHOLOGY

LISTA DE FIGURAS

- Fig. 1 Mapa de localização da área estudada. (A) Mapa da Bacia do Paraná e unidades sub e sobrejacentes. Destaque para as imagens B em vermelho e C em amarelo. (B) Detalhe da região estudada no estado do Paraná, próximo à Balsa Nova. (C) Detalhe da região estudada no estado do Mato Grosso do Sul, a nordeste da cidade de Aquidauana.....6
- Fig. 2 Carta Estratigráfica da Bacia do Paraná com destaque para o Grupo Itararé e Formação Aquidauana, foco do presente trabalho. (Adaptada de Milani et al. 2007).....8
- Fig. 3 Classificação proposta por Van der Meer (1993). Adaptado de Van der Meer & Menzies (2011).....16
- Fig. 4 Metodologia proposta por Phillips et al. (2011) para o mapeamento de tramas lineares17
- Fig. 5 Localization and simplified geology maps from study area. (A) Paraná Basin map with under and overlying units. Images B and C highlighted in red and yellow, respectively. (B) Detail of the studied area with described outcrops in Paraná state, next to Balsa Nova city. (C) Detail of the studied area with described outcrops in Mato Grosso do Sul state, northeast from Aquidauana city.21
- Fig. 6 Stratigraphic column of studied sucession from the Itararé Group (modified from Rosa et al. 2019), with stereograms referring to each glacial cycle and localization of thin sections.23
- Fig. 7 Structures observeds in glaciotectionized outcrops. (A) Open folds with metric amplitude and wave length in a diamictite rail road exposure from the Itararé Group. (B) Open folds with M, Z and S parasitic folds under striated pavement (C) from Aquidauana Formation. (D) Thrust with drag and rootless folds from Itararé Group outcrop.25
- Fig. 8 Itaré Group exposures in Paraná state. (A) Thrust with narrow shear zones (transport northwards). (B) Wavy sheared horizons, notice onlap of layers on the sheared plane on the left portion of the photo. (C) Detail of the sheared portion. Boudinaged sand layers in muddy matrix. (D) Striated pavement in Bassani quarry. (E) Faulted coarse sand layers in contact with stratified diamictite. Arrow indicates north. (F) Rotated clast in sandy diamictite with shadow pressure indicating dextral movement.26
- Fig. 9 Microstructures found in glacially deformed diamictites. Grain turbates in thin sections from the Itararé Group (A) sample BA11 and Aquidauana Formation (B) sample AQ15.3. Tight folds in diamictites from Paraná state (C and D), being C utilized as a dextral kinematic indicator (sample BA01). (E) Drag fold related to faults rupturing sand layer (sample BA01).28
- Fig. 10 Pseudo-foliations in glacially deformed samples. North to the right in all microphotographies. (A) Crenulated matrix from sample BA01 (S1, continuous black line) and crenulation cleavage (S2, black dashed line). Notice fluid scape structures (yellow arrows). (B) Crenulated detritic mica layers from sample BN03. (C) Skelsepic fabric in diamictites (BA10) and uniastrial plasmic fabric (BA06) (D). Shadow pressure around clasts from sample BA06 (E and F). Uniastrial plasmic fabric parallel to sample BN02-2 bedding with oblique cleavage fracture (G). Notice uniastrial fabric going around quartz grain. (H) Mica fish in sample BA06 indicating dextral movement.30
- Fig. 11 Shearing deatures and brittle deformation in diamictites. (A) Sheared matrix forming shadow pressures around quartz grain (sample BA11). Sheared grains in sand layer from sample BA01 (B and C). Sheared matrix going around grains in samples BA06 (D) and AQ15.3 (E). (F) Very fine sand layer in diamictite with normal faults, sample AQ15.3.....32

Fig. 12 Diagenetic features in glacially deformed rocks. (A) Concavo-convex and sutured grain contacts in quartz grains in sample BN03. (B) Stylolites in two different directions, with 90° angle between them – sample BA11. (C) Differential compaction in layers with and without matrix in sample PU02. (D) Cement partially dissolved in sample AQ15.3.34

Fig. 13 Linear trends map from sample AQ15. (A) High resolution scan from thin section in parallel nicols, highlighting clasts main compositions and structures found. (B) Referred polygons to the different mapped lineations, as well as shears, fluid escape structures and clasts bigger axis orientation. (C) Reliquary layering and shear structures. (D) Rose diagrams from the six thin sections from sample AQ15.36

Fig. 14 Linear trends map from sample BA06. (A) High resolution scan from thin section in parallel nicols, highlighting clasts main compositions and structures found. (B) Referred polygons to the different mapped lineations, as well as shears, fluid escape structures and clasts bigger axis orientation. (C) Main lineation trends. (D) Rose diagrams of mapped clasts, clasts alignments and shears.38

Fig. 15 - Linear trends map from sample BA10. High resolution scan from thin section in parallel (A) and crossed nicols (B), highlighting clasts main compositions and structures found. (C) Rose diagrams of mapped clasts, clasts alignments and shears.39

Fig. 16 Linear trends map from sample BA11. (A) High resolution scan from thin section in parallel nicols, highlighting clasts main compositions and structures found. (B) Referred polygons to the different mapped lineations, as well as shears, fluid escape structures and clasts bigger axis orientation.40

Fig. 17 Deformational structures from mass transport deposits from the Aquidauana Formation. Folds with different limbs openings: tight in section view (A), recumbent (B) and tight in plan view (C) associated to recumbent folds with intersection lineation (D). Hammer indicates north. (E) Thrust faults in clast poor diamictites from Aquidauana Formation. (F) Layered clast poor diamictite with reverse and normal faults. Notice that more intensively faulted areas become more homogenized.41

Fig. 18 Mass transport deposits with shear planes (A) that goes around apparently undeformed blocks (B). (C) Intra-stratal folds from Aquidauana Formation.42

Fig. 19 Microstructures described in thin sections from mass transport deposits. (A) Sand smearing in fault planes from poorly sorted stratified sandstone. Notice change in clast orientation, that become parallel to the normal fault (sample AQ17). (B) Crossed nicols scan of folded rock (recumbent fold), with fault nearly rupturing the superior limb. Sample AQ06. (C) Grain turbate (yellow) and multiple domains (blue) in diamictite. Sample AQ06. (D) Discrete pseudo- shadow pressure (yellow) surrounding quartz grain. Sample PU03. (E) Structure related to fluid escape in sample PU03. (F) Clay coating in polycrystalline quartz grain. Sample AQ20.44

Fig. 20 Linear trends map from sample AQ20. (A) High resolution scan from thin section in parallel nicols, highlighting clasts main compositions and structures found. (B) Referred polygons to the different mapped lineations, as well as shears, fluid escape structures and clasts bigger axis orientation. (C) Rose diagrams of mapped clasts, clasts alignments and shears.46

Fig. 21 (A) Sample PU03A with mapped faults and layering. (B) High resolution scan from thin section (PU03B) in parallel nicols, with mapped faults and layering. (C) Sample AQ17A with mapped faults and layering. (C) High resolution scan from thin section (AQ17B) in parallel nicols, with mapped faults and layering.47

Fig. 22 Stratigraphic column from Itararé Group (modified from Rosa et al. 2019) and rose diagrams of mapped clasts and shear structures.48

LISTA DE TABELAS

Tabela 1 – Coordenadas UTM dos afloramentos descritos durante as etapas de campo. Pontos em negrito indicam aqueles que foram selecionadas amostras para laminação 12

Tabela 2 – Microstructures described in thin sections from the Itararé Group and Aquidauana Formation 49

SUMÁRIO

CAPÍTULO 1 - INTRODUÇÃO

1.1	Introdução ao tema	1
1.2	Objetivos	4
1.3	Organização da dissertação	4
1.4	Área de estudo e contexto geológico	5
1.4.1	Late Paleozoic Ice Age (LPIA)	7
1.4.2	Bacia do Paraná	7
1.4.3	Grupo Itararé	8
1.4.4	Formação Aquidauana	10
1.5	Metodologia	12
1.5.1	Revisão bibliográfica	12
1.5.2	Atividades de campo	12
1.5.3	Micromorfologia	13

CAPÍTULO 2 – RESULTS (ARTICLE TO BE SUBMITTED TO THE JOURNAL *SEDIMENTOLOGY*) MICROMORPHOLOGY AS A TOOL FOR STUDYING DEFORMED PALEOZOIC SEDIMENTS

Abstract	17
2.1 Introduction.....	18
2.2 Geological context and study area	19
2.3 Methods.....	22
2.4 Results	23
2.4.1 Glacial-influenced deposits	24
2.4.2 Mass transport deposits.....	41
2.5 Discussion	48
2.5.1 Development and preservation of microstructures and linear trends in Paleozoic rocks	48
2.5.2 Influence of diagenesis	51
2.5.3 Are the fabrics described in thin sections correlated on a regional scale?	53
2.4.1 Structures in glacial (glaciotectonite) and gravitational (MTDs) deformed sediments.	55
2.6 Conclusion.....	56
2.7 References	57

CAPÍTULO 3 - CONSIDERAÇÕES FINAIS.....

REFERÊNCIAS

1. INTRODUÇÃO

1.1 Introdução ao tema

Durante muito tempo as deformações em sedimentos foi vista como ocorrências locais, sem significado no contexto geral de evolução estrutural de uma área, uma vez que o foco do estudo sobre a mecânica das rochas era em condições de alta pressão e temperatura, constantemente ignorando feições geradas em sedimentos. Porém, com a compreensão que estruturas geradas em material inconsolidado refletem uma gradação entre condições de subsuperfície e aquelas em maior profundidade, pesquisadores passaram a empenhar maior atenção nestas morfologias, empregando princípios e métodos utilizados na mecânica de solos (Maltman, 1994).

Os processos deformadores atuantes em sedimentos ocorrem em diferentes escalas e em diversos estágios antes da litificação completa do material, podendo ocorrer em diferentes ambientes geológicos. Maltman (1994) aponta ainda que uma grande gama de estruturas pode ser formada em resposta à força imposta, sendo em muitos casos semelhantes às aquelas formadas em condições de maior pressão e temperatura. O autor ainda identifica a diagênese como um “problema particular” para a deformação, reconhecendo que a evolução mineralógica do sedimento é um fator crítico para o comportamento deformacional.

Tendo quatro mecanismos de deformação principais (liquefação ou fluidização, gradação reversa de densidade, escorregamentos e cisalhamento), o processo de deformação gera produtos desde a micro até a macroescala. Para que ocorra a deformação em sedimentos, três condições precisam ser simultaneamente satisfeitas. Primeiro: uma força motriz (*driving force*) deve deformar feições sedimentares primárias; segundo: mecanismos de deformação devem permitir que o sedimento se deforme; terceiro: um gatilho que inicie os mecanismos de deformação (Owen *et al.*, 2011). As forças motrizes incluem a gravidade atuante no declive, instabilidades relacionadas à gradação inversa de densidade dos sedimentos, cisalhamento por correntes (aquosas ou outras), carga desigual de sedimentos e agentes químicos e biológicos (Owen *et al.*, 2011). Já os mecanismos de deformação são associados principalmente à “liquidização” (Allen, 1982), que envolve a mudança do comportamento do corpo de sólido para líquido

de forma rápida. A liquidação é um termo genérico utilizado pelo autor para abranger dois mecanismos distintos, a liquefação e fluidização. O primeiro ocorre quando o material granular bem selecionado e com empacotamento 'solto' colapsa totalmente como consequência do aumento da pressão de poros. Já a fluidização ocorre quando, de forma rápida, uma força empurra o fluido para cima através do corpo até que o peso imerso da massa de grãos seja igual ao arrasto causado pelo fluido (Owen *et al.*, 2011). Diferentemente da liquefação, a fluidização requer o influxo externo de fluido se movimentando para cima (Owen *et al.*, 2011).

Os gatilhos que dão início à deformação são objeto de estudo de diversos trabalhos (p. ex. Allen, 1982; Owen, 1987; Collinson, 1994; Moretti, 2000; Owen *et al.* 2011; Shanmugam, 2015; Shanmugam, 2016), podendo ser classificados como endógenos ou exógenos, abrangendo atividade sísmica, impactos de meteoros, ação de geleiras (glaciotectonismo), movimentos de massa, inundações, tempestades, eventos de sedimentação rápida, etc. Neste trabalho, serão estudados os produtos gerados por glaciotectônica e movimentos de massa.

A deformação glaciotectônica, isto é, deformação gerada pelo *stress* sobreposto por uma geleira no substrato, ocorre tanto em sedimentos inconsolidados quanto em material litificado. Este processo se dá sob ou na frente de grandes massas de gelo; em momentos de avanço, máximo glacial e até mesmo recuo dos glaciares. A descrição e interpretação das estruturas geradas (planos de cisalhamento, dobras, objetos rotacionados, *slickensides*, falhas, tramas, etc.) fornecem, assim como elementos geomorfológicos, importantes dados acerca do paleofluxo do gelo e a posição do material deformado em relação ao mesmo. O estudo da glaciotectônica ganhou destaque dentro da geologia estrutural e geomorfologia, principalmente quando se trata de sedimentos deformados no último período glacial durante o Pleistoceno. Há, no entanto, uma carência de trabalhos focados na parte deformacional de glaciações mais antigas, como a Paleozoica (p. ex. Le Heron *et al.*, 2005; Benn & Prave, 2006; Busfield & Le Heron, 2013, 2018; Fedorchuk *et al.*, 2019). Processos relacionados a ambientes glaciais também podem produzir estruturas em sedimentos inconsolidados, como movimentos

em massa (subaquáticos ou subaéreos), “arraste” de quilhas de *iceberg* e a liberação de detritos por gelos flutuantes.

Já os movimentos de massa geram depósitos por fluxos gravitacionais coesos a partir de processos de ressedimentação (Martinsen, 1994). Compondo grande parte de sucessões estratigráficas marinhas profundas, atingindo valores superiores a 50% segundo Posamentier & Walker (2006). O estudo de tais depósitos é de grande relevância em diversos aspectos, até mesmo para a exploração de hidrocarbonetos (uma vez que reservatórios podem estar condicionados aos depósitos, Posamentier & Martinsen, 2011). A análise estrutural, assim como a análise estratigráfica, de paleotalude e de características morfológicas, de *mass transport deposits* - MTDs vem sendo abordada por diversos autores (p. ex. Eyles & Eyles, 2000; Martinsen *et al.*, 2003; Alsop & Marco 2011, 2013, Alsop *et al.*, 2017; Ogata *et al.*, 2014; Sobiesiak *et al.*, 2016, Rodrigues *et al.* 2020). Destacam-se ainda trabalhos sobre movimentos de massa no Grupo Itararé da Bacia do Paraná (p.ex. Gama Jr. *et al.*, 1992; Vesely *et al.*, 2015; Suss *et al.*, 2014; Mottin *et al.*, 2018; Schemiko, 2019), especialmente o trabalho de Rodrigues *et al.* (2020) que descreve do ponto de vista estrutural depósitos de movimento em massa e como a orientação das estruturas podem auxiliar na definição de paleotaludes. Os autores descrevem dobras cilíndricas suaves a cerradas, dobras de arrasto, falhas de geometrias variadas, *boudins*, injectitos e estruturas de cisalhamento compondo diferentes fácies deformacionais. Tais fácies são individualizadas a partir da porcentagem de matriz no depósito, resultado do aumento da deformação, desagregação e mistura dos sedimentos, gerando rochas cada vez mais homogêneas (Rodrigues *et al.*, 2020).

Além das estruturas geradas em escala macro e mesoscópica, feições observadas em lâmina podem auxiliar no entendimento da deformação sofrida pelas rochas analisadas. Para rochas deformadas em ambientes glaciais, Van de Meer (1993) classifica essas microfeições entre “*plasmic fabrics*” e “*S-matrix microstructures*” e suas subdivisões, de acordo com a ocorrência de elementos <25-30 μm (plasma) e maiores que 35 μm (*skeleton grains*). Além da classificação proposta, Phillips *et al.* (2011) desenvolveram um método a partir do ‘mapeamento’ da orientação dos eixos maiores

dos clastos vistos em lâmina, permitindo individualizar diferentes tramas (ou pseudo-foliações) imperceptíveis de outra forma. Assim, a caracterização estrutural de rochas (principalmente tilitos e diamictitos) aparentemente homogêneas pode ser conduzida, ampliando a fonte de informação cerca dos depósitos estudados.

1.2 Objetivos

O escopo deste estudo é caracterizar estilos deformacionais, principalmente do ponto de vista microscópico, em rochas deformadas antes de sua consolidação em ambientes glaciais ou glacio-relacionados e em depósitos de transporte em massa. Busca-se afirmar se há ou não diferenças nas estruturas geradas a partir de diferentes agentes deformacionais (gravidade – depósitos de transporte em massa; gelo – depósitos glacio-influenciados). Além disso, busca-se avaliar a preservação de microestruturas após a diagênese dos sedimentos deformados, uma vez que as classificações utilizadas na literatura foram baseadas em sedimentos recentes, nos quais houve pouca ou nenhuma ação de processos diagenéticos.

Para tanto, os objetivos específicos são:

- Documentar e classificar estruturas deformacionais em macro, meso e micro escala;
- Comparar feições de deformação relacionadas com diferentes ambientes deformacionais;
- Descrever feições diagenéticas;
- Avaliar o impacto da diagênese na obliteração da microtrama.

1.3 Organização da dissertação

A estrutura da dissertação se dá por três capítulos, sendo eles:

- Capítulo 1 - Introdução ao tema abordado, objetivos da pesquisa, área de estudo, contexto geológico em escalas regionais e locais, e por fim, revisão dos conceitos e métodos aplicados no trabalho;

- Capítulo 2 – Resultados e discussões obtidos, sendo estes apresentados em formato de artigo para posterior submissão em revista científica internacional (*Sedimentology*). As figuras e tabelas do artigo possuem numeração sequencial diferente à dissertação e as referências utilizadas no artigo podem ser encontradas no item 2.6;
- Capítulo 3 - Considerações finais sobre a pesquisa.

1.4 Área de estudo e contexto geológico

Este estudo foi desenvolvido em rochas permocarboníferas da Bacia do Paraná, expostas tanto na borda leste (Grupo Itararé) quando na borda oeste (Formação Aquidauana), formadas durante a *Late Paleozoic Ice Age* (LPIA). Na borda oriental a seção estudada localiza-se próximo aos municípios de Balsa Nova e Campo do Tenente (Paraná), enquanto os afloramentos da borda ocidental estão localizados próximos aos municípios de Aquidauana, Rochedo e Corguinho (Mato Grosso do Sul; fig.1)

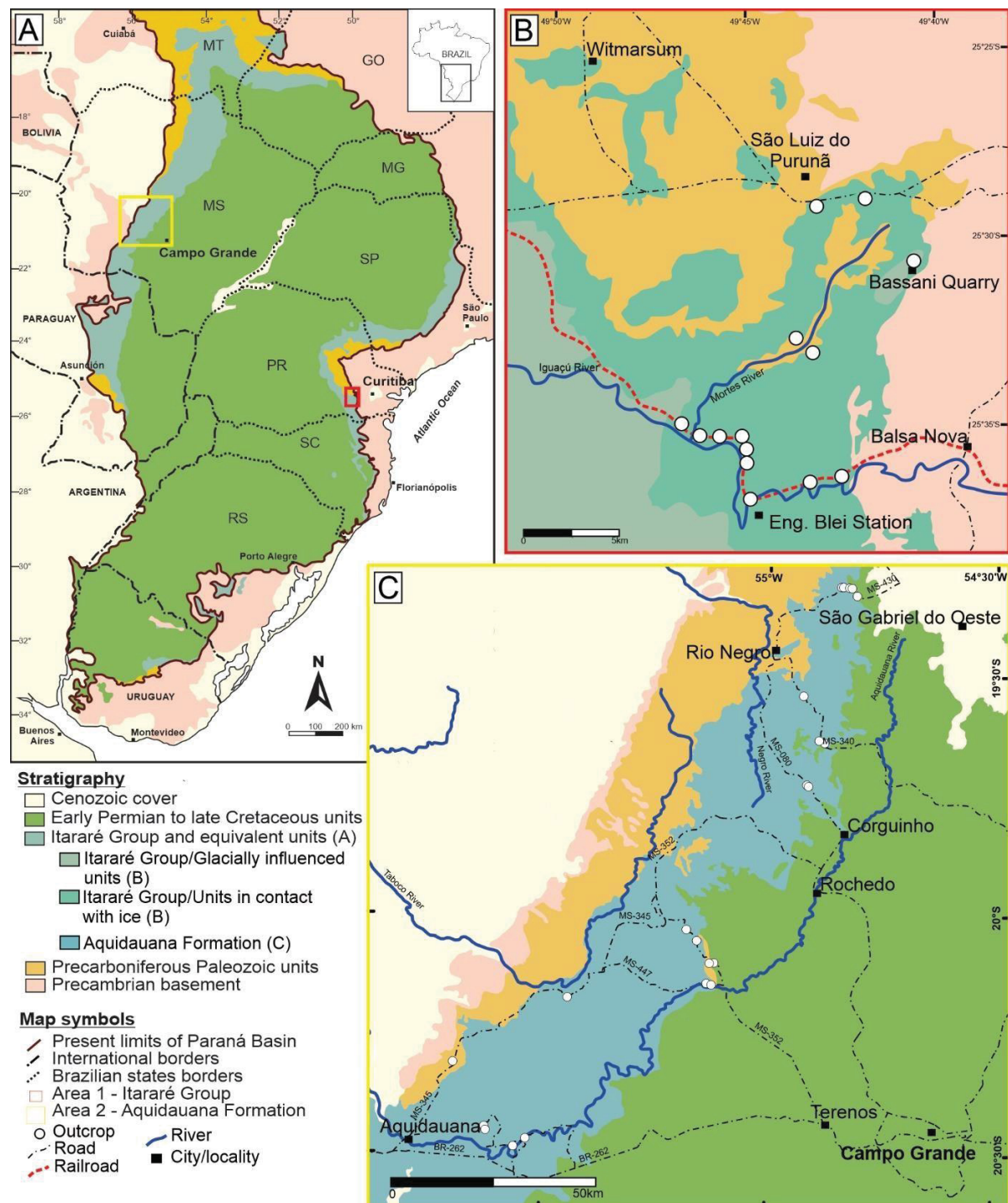


Fig. 1 Mapa de localização da área estudada. (A) Mapa da Bacia do Paraná e unidades sub e sobrejacentes. Destaque para as imagens B em vermelho e C em amarelo. (B) Detalhe da região estudada no estado do Paraná, próximo à Balsa Nova. (C) Detalhe da região estudada no estado do Mato Grosso do Sul, a nordeste da cidade de Aquidauana.

1.4.1 Late Paleozoic Ice Age (LPIA)

A documentação de glaciações no registro estratigráfico é dada através de aspectos erosivos, deposicionais e deformacionais, formados pelas interações diretas ou indiretas de geleiras. Tais aspectos podem ser relacionados a relevos erosivos, tilitos subglaciais e depósitos glaciectonizados, além de depósitos subaquosos que compreendem “grounding-lines fans”, *ice rafts debris* (IRD) e material glacial ressedimentado. O período glacial melhor compreendido é a Glaciação do Paleozoico Superior (LPIA), com registro sedimentar em bacias do Gondwana de altas e médias paleolatitudes (Isbell *et al.* 2003). Seu registro compreende depósitos marinhos e depósitos com influência glacial indireta, sendo raros os casos de registros com influência direta da geleira. Devido ao intemperismo pós deposicional e à grande cobertura de sedimentos de deglaciação, a abordagem geomorfológica comumente usada para reconstruir sistemas glaciais cenozoicos (Darvill *et al.* 2017) é de difícil aplicação para a LPIA. Formas erosivas subglaciais são as feições mais confiáveis e usadas para a interpretação da cinemática da geleira, além disso estruturas glaciectônicas desenvolvidas em contextos subglaciais e marginais (em relação ao gelo) são de importante uso para a determinação tanto da cinemática quanto da extensão das geleiras (Rosa *et al.* 2016).

1.4.2 Bacia do Paraná

A Bacia do Paraná é uma extensa cobertura sedimentar e vulcânica intracratônica, abrangendo grande parte do sul, centro-oeste e sudeste brasileiro, bem como leste do Paraguai e nordeste da Argentina, totalizando cerca de 1.500.000km² de área e até 7000 metros de espessura. Milani (1997) reconheceu na bacia seis sequências de segunda ordem ou supersequências (Vail *et al.*, 1977), separadas por hiatos deposicionais. São elas: Rio Ivaí (Ordoviciano – Siluriano), Paraná (Devoniano), Gondwana I (Carbonífero - Eotriássico), Gondwana II (Meso - Neotriássico), Gondwana III (Neojurássico - Eocretáceo) e Bauru (Neocretáceo). As três primeiras sequências foram interpretadas por Milani *et al.* (2007) como ciclos de transgressão e regressão ocasionados pela entrada marinha na Bacia do Paraná durante o Paleozoico. Já as demais três correspondem a um registro sedimentar continental, com rochas vulcânicas associadas.

1.4.3 Grupo Itararé

O Grupo Itararé abrange um registro espesso da LPIA, com aproximadamente 1300 metros de uma sucessão que vai desde o Baskiriano Superior até o Sakmariiano Inferior (fig. 2), composta por rochas sedimentares depositadas em contexto glacial largamente reconhecido na literatura, desde as suas primeiras menções e descrições, como em Derby (1878, citado por Gama Jr *et al.*, 1992), Oliveira (1927, citado por Schneider *et al.*, 1974) e Gordon Jr. (1947, citado por Schneider *et al.*, 1974).

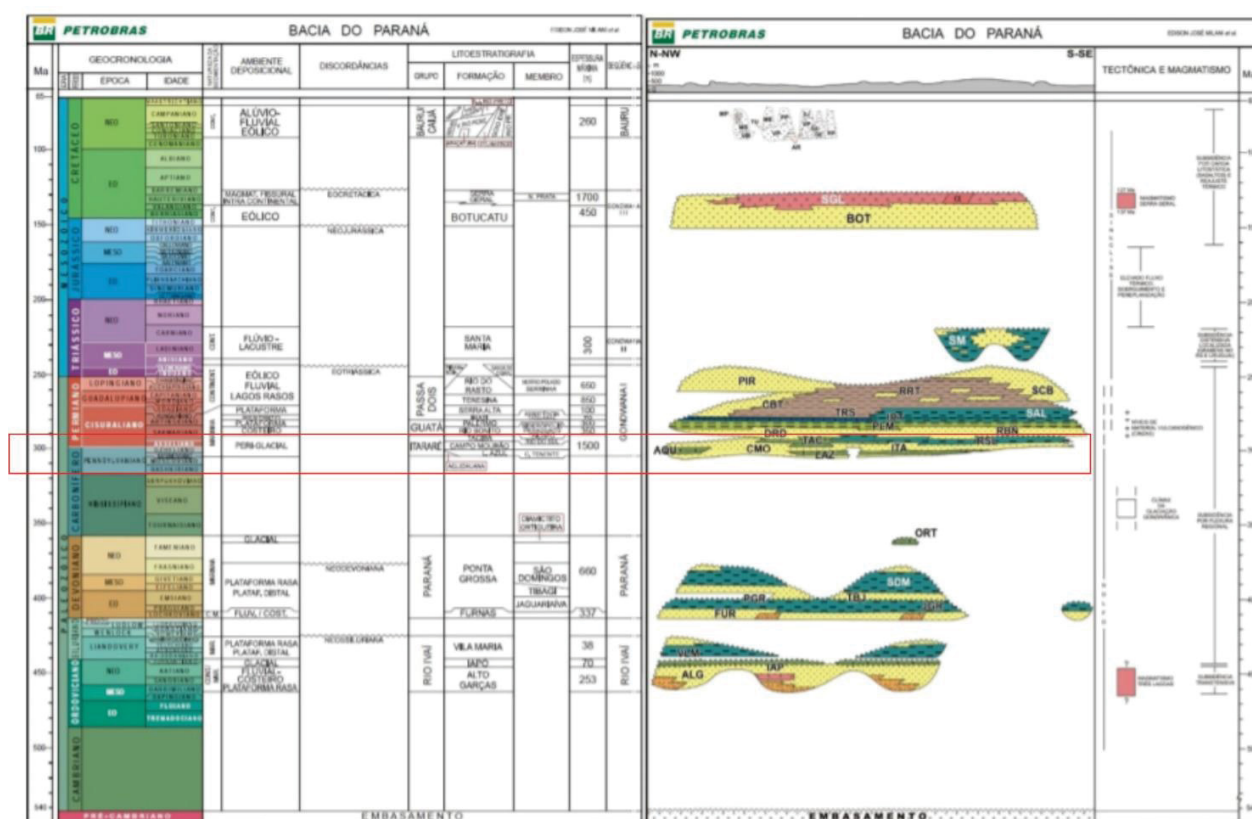


Fig. 2 Carta Estratigráfica da Bacia do Paraná com destaque para o Grupo Itararé e Formação Aquidauana, foco do presente trabalho. (Adaptada de Milani *et al.* 2007)

Schneider *et al.* (1974) propuseram para o Grupo uma divisão em quatro formações, sendo elas: Campo do Tenente, Aquidauana, Mafra e Rio do Sul, da base ao topo, respectivamente. A Formação Aquidauana poderia ser encontrada no Mato Grosso, Goiás e nordeste de São Paulo, enquanto as restantes haviam sido mapeadas até o momento em Paraná e Santa Catarina. Os autores descrevem uma sucessão de rochas sedimentares variadas, pelíticas e psamíticas, com relativa abundância de diamictitos ao

longo de sua exposição, o que refletiria influências do contexto glacial regional. Divisões estratigráficas mais atuais do Grupo mantiveram similaridades com o trabalho de Schneider *et al.* (1974), mas apresentam avanços cruciais, incluindo dados de datação.

França & Potter (1988) reconheceram outras formações do registro do Grupo Itararé, com variações em relação à posição na Bacia do Paraná em que afloram. Os autores reconhecem as formações Lagoa Azul, Campo Mourão e Taciba referentes a três ciclos deposicionais controlados por mudanças climáticas e do nível do mar.

Segundo os autores, a unidade basal do Grupo Itararé, a Formação Lagoa Azul - que ocorre principalmente em São Paulo e Paraná - pode ser dividida em um membro psamítico (Cuiabá Paulista) e outro membro pelítico (Tarabáí), sendo o último interpretado como produto da sedimentação glaciogênica direta. A Formação Campo Mourão, por sua vez, teria ocorrência ampla na Bacia do Paraná, estando ausente apenas no registro de algumas porções do Rio Grande do Sul, estando em contato concordante com a unidade subjacente. Esta formação, predominantemente arenosa, é subdividida em um Membro Lontras no sudeste de Santa Catarina, onde aflora uma sequência contínua de folhelhos cinza escuros. Em contato concordante com a Fm. Campo Mourão (ou discordante com o próprio embasamento, próximo ao Arco Sul Rio-

Grandense), França & Potter (1988) subdividiram a Formação Taciba em Membros Rio Segredo, Chapéu do Sol e Rio do Sul. Para os autores, a maior parte da área de afloramento do Grupo Itararé na Bacia do Paraná compreende sedimentos desta formação, sendo que o Membro Rio Segredo apresentaria interdigitações com os arenitos avermelhados da Formação Aquidauana. Acima do Rio Segredo estão os Membros Chapéu do Sol e Rio do Sul, em contatos laterais e interdigitados, o último com origem na Formação Rio do Sul de Schneider *et al.* (1974). Segundo França & Potter (1988), as formações Campo do Tenente e Mafra de Schneider *et al.* (1974) podem ser correlacionadas com a Formação Campo Mourão.

Sobre o Membro Rio do Sul, França & Potter (1988) descrevem um ambiente deposicional marinho profundo, reconhecido também em Schneider *et al.* (1974), graças a presença de fósseis típicos como braquiópodes, crinóides, foraminíferos, orbiculoides, entre outros. Estes mesmos pesquisadores também já assumiam que os “seixos pingados” em folhelhos da Formação Rio do Sul deveriam ter sido transportados e depositados por *icebergs*, visão seguidamente corroborada por autores de tempos mais recentes, como Eyles *et al.* (1993). O Mb. Rio do Sul, segundo França & Potter (1988) representa a transgressão da Bacia do Paraná de sul para norte, onde, por sua vez, está registrado o Membro Chapéu do Sol. Nesta região deveriam existir geleiras marinhas, sendo possivelmente responsáveis pela deposição de alguns dos diamictitos desta unidade, enquanto que outros poderiam ser fácies ressedimentadas por movimentos de massa, como reconhecido posteriormente por autores como Gama Jr. *et al.* (1992) e Eyles *et al.* (1993).

Gama Jr. *et al.* (1992) citam a abundância de fácies de ressedimentação intercaladas a fácies marinhas e costeiras no Grupo Itararé, que abrangem, além dos diamictitos, também ritmitos e arenitos, como fácies oriundas do retrabalhamento dos depósitos glaciogênicos (tilitos). Desta forma, os autores sugerem que os fluxos gravitacionais sejam os mais importantes agentes deposicionais deste contexto, cujos produtos teriam uma importância volumétrica consideravelmente maior que a dos produtos da sedimentação primária glacial.

É importante ressaltar que diversos autores, como Gama Jr. *et al.* (1992), Eyles *et al.* (1993) e Canuto (1993) reconheceram associações faciológicas que permitem inferir que os processos de sedimentação dominantes no Grupo Itararé foram, de maneira geral, o “*rain-out*” (chuva de detritos), a ressedimentação em declives, os fluxos gravitacionais, as correntes de turbidez e o *outwash*, além de secundariamente deposição glacial em forma de tills, em ambientes glacio-continentais e glacio-marinhos. A análise das complexas associações de fácies e sequências sedimentares desta unidade moldaram interpretações mais aprofundadas e bem fundamentadas de paleoambientes deposicionais; que são, entretanto, distintas entre si.

1.4.4 Formação Aquidauana

A Formação Aquidauana, de ocorrência restrita ao norte da Bacia do Paraná, compreende três sequências principais, tanto para Schneider *et al.* (1974) quanto para França & Potter (1988), sendo a basal e a superior de arenitos e a intermediária de siltitos e lamitos seixosos avermelhados, com espessura máxima de 799 metros. Estas camadas, como referido anteriormente, encontram-se em interdigitação com outras rochas do Grupo Itararé no centro-sul da Bacia do Paraná, sendo equivalentes, do ponto de vista temporal, ao Grupo. A distinção entre as sequências pertencentes ao Grupo Itararé e à Formação Aquidauana se dá simplesmente pela cor avermelhada das rochas da Formação, que foi definida tanto em dados de superfície e subsuperfície (França & Potter, 1988). Mesmo sendo correlatas e sido depositadas durante a *Late Paleozoic Ice Age*, os ambientes deposicionais e área fonte de sedimentos são considerados distintos para a Formação Aquidauana dos do Grupo Itararé.

Apesar de considerada como Grupo por alguns autores (Rocha-Campos, 1967; Rocha-Campos & Santos, 1981), a classificação como ‘Formação’ Aquidauana é amplamente aceita na comunidade científica. Devido à ausência de camadas que permitem correlações regionais e poucos dados concisos a respeito de idades, a estratigrafia da Formação Aquidauana ainda não é bem compreendida. Trabalhos datados desde a década de 50 (p. ex. Beurlen, 1956; Petri & Fúlfaro, 1966; Farjallat, 1970) descrevem rochas de deposição glaciogênica direta (tilitos), além de arenitos pré e pós glaciais.

Schneider *et al.* (1974) sugerem condições continentais, fluviais e lacustres, com influência subordinada de deposição glaciogênica para os ambientes sedimentares da Formação, que foi subdividida pelos autores em três intervalos: inferior (composto principalmente por arenitos, com diamictitos, lamitos e conglomerados subordinados); intermediário (siltitos, folhelhos e diamictitos); e superior (constituído principalmente por rochas arenosas). Gesicki (1996) e Gesicki *et al.* (1998) subdividiram a Formação Aquidauana no estado do Mato Grosso do Sul também em membros inferiores, intermediários e superiores, utilizando como critério mudanças no nível do mar. Tais membros podem ser correlacionados parcialmente às Formações Lago Azul, Campo Mourão e Taciba de França & Potter (1988).

Os trabalhos de Gesicki (1996) e Gesicki *et al.* (1998) descrevem ainda ambientes deposicionais para cada membro, sendo: membro inferior depositado em sistemas de leques aluviais e rios entrelaçados, com retrabalhamento eólico localizado; membro intermediário caracterizado por correntes de turbidez de baixa densidade *offshore*, relacionadas a um aumento do nível do mar durante o período interglacial; e superior depositado por fluxos trativos de alta energia em lâmina d'água rasa, com intensa ressedimentação e aumento da exposição subárea em direção ao topo da sequência. Na porção superior da Formação Aquidauana ainda são caracterizados depósitos com forte influência eólica e lacustrina, com participação discreta da deposição de sal (Gesicki, 1996), que não possuem evidência de deposição relacionada à ambientes glaciais.

A influência glacial nas rochas da Formação Aquidauana é observada apenas em sua porção inferior, onde superfícies estriadas, diamictitos e conglomerados com clastos facetados e estriados foram documentados (Caster, 1947; Almeida, 1954; Petri e Fúlfaro, 1966; Guirro, 1991; Gesicki, 1996). São descritos ainda *dropstones* e feições de corte e preenchimento. Apesar de interpretadas como estrias glaciais por Gesicki *et al.* 2002, o pavimento estriado sobre arenitos devonianos da Formação Furnas foi posteriormente considerado como resultado do arraste de quilhas de *icebergs* no substrato.

1.5 Metodologia

Os métodos utilizados para a elaboração desta pesquisa foram: revisão bibliográfica, aquisição de dados e amostras de campo, tratamento e interpretação dos dados a partir de lâminas petrográficas.

1.5.1 Revisão bibliográfica

O trabalho iniciou-se com um levantamento bibliográfico focado tanto na geologia local quando na metodologia a ser aplicada para obter os resultados esperados, visando tópicos como: geologia da Bacia do Paraná, deformação de sedimentos, deformação de sedimentos em ambientes glaciais e em MTDs, micromorfologia de sedimentos, feições diagenéticas, entre outros.

1.5.2 Atividades de campo

Durante seis campanhas de campo, 38 afloramentos foram descritos entre os estados do Mato Grosso do Sul e Paraná, abrangendo principalmente cortes de estradas e ferrovias, cavas e drenagens, onde ocorreriam as melhores e menos intemperizadas exposições (tabela 1). Foram coletados dados estruturais (DIP_DIR/DIP) referentes a falhas, dobras e feições de cisalhamento, além de amostras orientadas para a confecção de lâminas delgadas de diferentes dimensões (2,5 x 4,5cm e 5 x 7,5cm). As litologias foram descritas e correlacionadas com as fácies descritas por Rosa *et al.* (2019) e Gesicki (1996). Além disso, fotos dos afloramentos mais importantes foram tiradas para a montagem e interpretação de fotomosaicos com o *software* Panavue.

Tabela 1 – Coordenadas UTM dos afloramentos descritos durante as etapas de campo. Pontos em negrito indicam aqueles em que foram selecionadas amostras para laminação.

PONTO	ZONA	UTM OESTE	UTM SUL
FORMAÇÃO AQUIDAUANA			
AQ01	21S	643845	7738004
AQ02	21S	643746	7738559
AQ03	21S	653215	7735709
AQ04	21S	640428	7733862
AQ05	21S	644002	7737649
AQ06	21S	636561	7753450
AQ07	21S	663017	7768276
AQ08	21S	696871	7776119

AQ09	21S	692953	7781256
AQ10	21S	690570	7783833
AQ11	21S	695824	7776020
AQ12	21S	695145	7771377
AQ13	21S	718820	7816828
AQ14	21S	726950	7862902
AQ15	21S	696291	7771032
AQ16	21S	726530	7862907
AQ17	21S	718405	7817165
AQ18	21S	728315	7862774
AQ19	21S	717712	7837769
AQ20	21S	754175	7833617
AQ21	21S	722583	7826839
AQ22	21S	721258	7827458
AQ23	21S	730078	7860869
AQ24	21S	730322	78060590
GRUPO ITARARÉ			
BN01	22S	628801	7175136
BN02	22S	626138	7169845
BN03	22S	626372	7169231
BN04	22S	630499	7168169
BN05	22S	626204	7168423
BN06	22S	626192	7169786
BN07	22S	625890	7170091
BN08	22S	623583	7170371
BN09	22S	622904	7170829
BN10	22S	621962	7171432
PU02	22S	631729	7182190
PU03	22S	629724	7181744
BA	22S	633796	7178462
EB	22S	626983	7167080

1.5.3 Micromorfologia

Utilizando microscópios de luz transmitida, 31 lâminas foram descritas e analisadas sob perspectivas micromorfológicas, microssedimentares e diagenéticas. Em quanto a microssedimentologia estuda a relação entre as partículas e as variadas estruturas sedimentares, a micromorfologia examina a relação entre elementos microscópicos e “artefatos” sedimentares relacionados (Menzies & Meer, 2017).

O estudo integrado de macro e microfábricas é utilizado para fornecer evidências sobre o paleofluxo do gelo, discriminar diamictitos de diferentes ambientes glaciais sedimentares e para modelar o comportamento de tilitos sob *stress* subglacial. A análise micromorfológica em sedimentos glaciais foi evoluída a partir de classificações taxonômicas desenvolvidas inicialmente no contexto da micropedologia (van der Meer, 1987, 1996; van der Meer *et al.*, 2003; Carr, 2004). Desde então, trabalhos consistentes que datam desde a década de 50 (p. Ex. Sitler & Chapman, 1955; Sitler, 1968) foram rapidamente evoluídos durante a década de 70 com o surgimento da resina *epoxy*, que facilitou a confecção de lâminas delgadas. Trabalhos mais recentes, a partir dos anos 1990, trazem classificações acerca das estruturas encontradas, dividindo-as em *plasmic microfabric* e *S-matrix*, onde o critério para tal divisão é a presença de componentes individualizáveis dentro da resolução do microscópio ótico (~30um) (Van der Meer, 1993). A presença de tramas plasmáticas indica a ocorrência de partículas ou agregados de argila que exibem birrefringência no microscópio óptico (Zaniewski, 2001). Essas tramas, características de deformações plásticas, são classificadas em *Lattisepic*, *Omnisepic*, *Uniastrial* e *Insepic* de acordo com o tipo e grau de orientação das partículas. *Insepic*, *Lattisepic* e *Omnisepic* correspondem a birrefringências aleatórias, suaves a fortes respectivamente, enquanto tramas uniastriais são orientações únicas bem marcadas. Plasmas bandados, por sua vez, indicam mistura incompleta de fácies diferentes de sedimentos (Van der Meer & Menzies, 2011). A identificação destas tramas é importante pois seus padrões são indicativos da direção do *stress* aplicado sobre o material: enquanto estruturas paralelas ao acamamento indicam que o esforço principal foi causado por sobrecarga, tramas em ângulo com o acamamento indicam geração por cisalhamento (Bordonau & van der Meer, 1994).

Já as estruturas formadas por *skeleton grains* são divididas a partir do seu comportamento quando deformadas, sendo agrupadas em dúcteis (neste trabalho referidas como plásticas), rúpteis, polifásicas (rúptil-dúctil) e estruturas induzidas por escape de fluidos (Maltman, 1994; Passchier & Trouw, 1996; Menzies, 1998) (fig. 2). Tais estruturas fornecem informações importantes cerca de processos complexos pré-, sin- e pós-deposicionais. Estruturas compostas por *plasmic fabrics* e *skeleton grains* são

denominadas como *skelsepic plasmic fabrics*, onde o plasma orientado pode ser observado contornando grãos individuais.

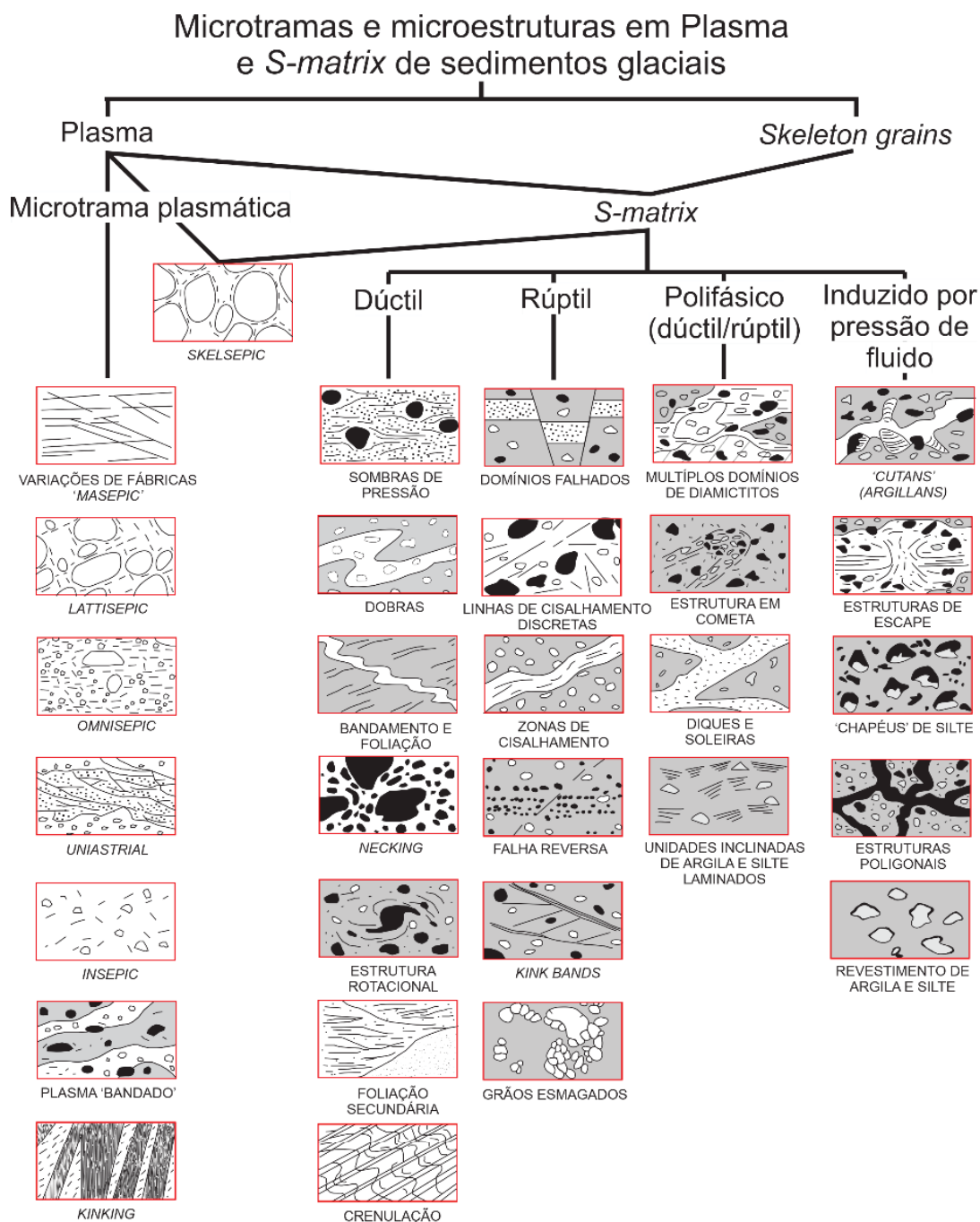


Fig. 3 Classificação proposta por Van der Meer (1993). Adaptado de Van der Meer & Menzies (2011)

Essa classificação de estruturas, porém, tende a ignorar o desenvolvimento potencial de diversas fases de microfábricas. O método proposto por Phillips *et al.* (2011) utiliza a orientação do maior eixo de grãos detríticos (*skeleton*) em diamictitos, identificando *trends* principais (ou tramas lineares/lineações) e permitindo a delimitação de domínios de microfábricas a partir da orientação preferencial de grãos alongados (fig. 3). Para isto, cinco etapas são necessárias e foram cumpridas neste trabalho: 1) importar um *scan* de alta resolução da lâmina em um *software* de design gráfico (p.ex. CorelDRAW); 2) aumentar a imagem para que grãos de areia fina fiquem visíveis e, em uma camada separada, digitalizar os eixos maiores dos *skeleton grains*. Digitalizar demais estruturas que forem relevantes e contribuïrem com a interpretação do ‘mapa’ de microestruturas; 3) exportar os dados referentes aos eixos e plotá-los em *softwares* de análise estrutural; 4) com um estilo diferente de linha, definir as tramas preferenciais a partir de três ou mais clastos alinhados entre si; 5) identificar domínios de microtramas interpretar a lâmina microestruturalmente.

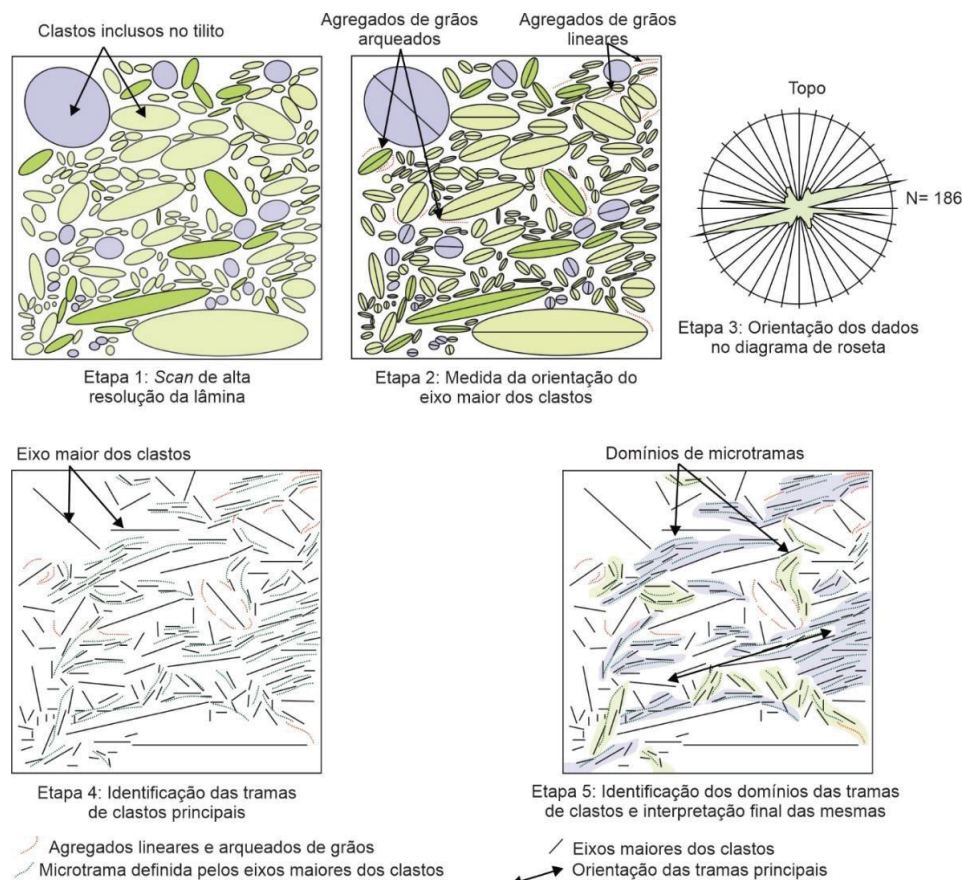


Fig. 4 Metodologia proposta por Phillips *et al.* (2011) para o mapeamento de tramas lineares

2. RESULTS (ARTICLE TO BE SUBMITTED TO INTERNATIONAL JOURNAL)

MICROMORPHOLOGY AS A TOOL FOR STUDYING DEFORMED PALEOZOIC SEDIMENTS

Abstract

The Late Paleozoic Ice Age (LPIA) is represented in the Paraná Basin through the time equivalent units of Itararé Group and Aquidauana Formation. These sedimentary rocks provide an extensive glacial record, containing deformed intervals interpreted as glacioteconites and mass-transport deposits (MTD), combined with undeformed successions. Glacioteconized deposits have features such as folds, thrusts and shear zones, which could be subglacial or proglacial produced. Furthermore, in a similar way, MTD have structures caused by shearing, compression, and distension. Few studies have addressed microscale structures related to sediment deformation from the Paleozoic - or even older periods -, generated by glacioteconic or gravitational deformation, which can be obliterated by subsequent diagenetic processes. This study aims to address this issue and correlate the range of microstructures present in the petrographic thin section to different depositional and deformational settings, interpreted based on the macroscopic description of sedimentary facies. The results are used to critically assess the applicability of micromorphology in distinguishing paleoenvironments in the Pre-Pleistocene glacial record, and how these structures can be modified over time in response to lithification and diagenesis. The study combines field data with detailed micromorphological and microstructural analysis of 40 thin sections from the Itararé Group and Aquidauana Formation. Samples were collected from a range of lithotypes from different settings, including diamictites, sandstones and mudstones from mass transport, and subglacial and proglacial glacioteconism. The microstructures present include unistrial plasmic fabrics, rotational structures, microshear zones, sheared clasts, faults, folds, 'boudins' and intraclasts. However, in some well-sorted facies, which contain little or no matrix, also containing features typically associated with compaction and diagenesis, such as grain crushing, reduction of primary porosity, sutured contacts and stylolites. Results show that sediments from a range of different depositional settings may contain a similar assemblage of microstructures. This suggests that microstructures alone cannot fully characterize the depositional environment in older sequences. In addition, diagenesis plays a major role in the preservation of primary sedimentary structures and soft-sediment deformation features, which may lead to the overlapping of these structures if the rock has a low amount of matrix.

2.1 Introduction

2.2 Geological context and study area

The Paraná Basin is an intracratonic basin located in South America, covering part of Argentina, Paraguay, Uruguay, and Brazil with an area of approximately 1,600,000 km² (fig. 05A). Established after the magmatic and metamorphic events of the Brasiliano Cycle (Almeida and Hasui, 1984), the basin has a polycyclic tectono-sedimentary evolution, with sedimentary successions divided into two depositional cycles separated by erosional unconformities (Milani, 2004). The first cycle consists of Siluro-Devonian deposits from the Paraná Group while the latter is represented by the Permo-Carboniferous groups of Itararé, Guatá and Passa Dois.

The Itararé Group covers a thick record of the Late Paleozoic Ice Age - a glacial period best understood in the geologic record, preserved in Gondwana basins of medium and high paleolatitudes (Isbell et al., 2003) -, with approximately 1300 meters of a rocky succession that goes from the Upper Bashkirian to the Lower Sakmarian. The record is formed mainly by mass transport deposits, turbidites, and outwash plains and alluvial fans, interpreted as large deglaciation cycles, in a stratigraphic stacking represented by a retrogradational sequence, with sandy and gravelly intervals at the base and pelitic intervals in the top (France and Potter, 1998; Vesely and Assin, 2004). The succession studied within the Group belongs to the most basal formation, defined by França and Potter (1988) as Lagoa Azul, set in erosive contact over the Furnas Formation sandstones and metamorphic rocks of the Precambrian basement. In the studied region, the sequences, which add up to 80m in thickness, were informally subdivided by Rosa et al. (2019) based on facies and stratigraphic characteristics, deformation styles and direction of paleo ice flow indicators. The boundaries between them are marked by erosion surfaces and abrupt changes in the intensity of the deformation (the maximum deformation is found at the top of the sequences) (Rosa et al., 2019). Structurally, symmetrical and asymmetrical folds are described, with gaps between varied members, from smooth to closed and isoclinal, low-angle thrusts and millimeter-to-centimeter subhorizontal shear planes, with overall slope varying according to the unit: north in 1A; west in lower and middle 1B; and northwest in upper 1B (Rosa et al, 2019). Axes of isoclinal folds with an eastward slope are also

measured in the lower 1B unit, and the ice flow is inferred by glaciotectonic and erosive kinematic indicators, composing three cycles of advance and retreat of the ice in the region. They are: GC1, represented by unit 1A and moving north; GC2, composed of the lower and middle units 1B and moving to the south-southwest, with small fluctuations in the ice margin characterizing two subordinate cycles (GC2-A and GC2-B); and G3, related to the upper 1B sequence and moving northwest.

On the opposite edge of the basin, in the states of Mato Grosso, Mato Grosso do Sul and Goiás, in addition to Paraguay, outcrop the rocks of the Aquidauana Formation (fig.05A) with up to 700 meters. Interpreted as a temporary correlate to the Itararé Group, the Formation is distinguishable from it mainly by the reddish color of its rocks, a characteristic observed both in outcrop and subsurface (França and Potter, 1988). Despite the temporal correlation (both the Aquidauana Formation and the Itararé Group would have been deposited during the Late Paleozoic Glaciation), it is understood that the rocks of the Aquidauana Formation are distinct from the point of view of the deposition environments and source area of the glaciers. Nevertheless, the scarcity of stratigraphic layers of regional correlation and low resolution age data, the stratigraphy of the Formation and how its layers are related to those found in the Itararé Group is restricted, with several proposals made so far. In this context, the work of Gesicki (1996) and Gesicki et al. (1998) stand out, which informally subdivides the Formation in the lower, middle and upper Mato Grosso do Sul areas, characterized mainly by changes in sea level, which may be partially correlated with Lago Azul, Campo Mourão and Taciba Formations (França and Potter, 1988).

The lower member of Gesicki et al. (1998) represents intertwined river systems and alluvial fans with little wind rework, laterally grading to shoreface and onshore deposits related to storm rework and confined and unconfined re-sedimentation, possibly caused by glacier advance. The middle member, on the other hand, is characterized by an interglacial stage with extensive flooding and fine material sedimentation, caused by low-density tumultuous processes under warmer weather. Finally, the upper member represents a new phase of glacial advance into the basin, marked by deposition in shallow waters by flows of high tractive energy, intense re-sedimentation, and greater subaerial exposure towards the top. From striated pavements, the predominant direction of the ice is inferred towards

north-northwest. As for deformational structures, Gesicki (1996) mainly describes brittle structures, such as faults and clastic dikes, featuring five deformational phases (1- EW extension, 2- dextral shear, 3- EW compression, 4- NE-SW compression, 5- EW extension). Groups of folds and overload structures are also described.

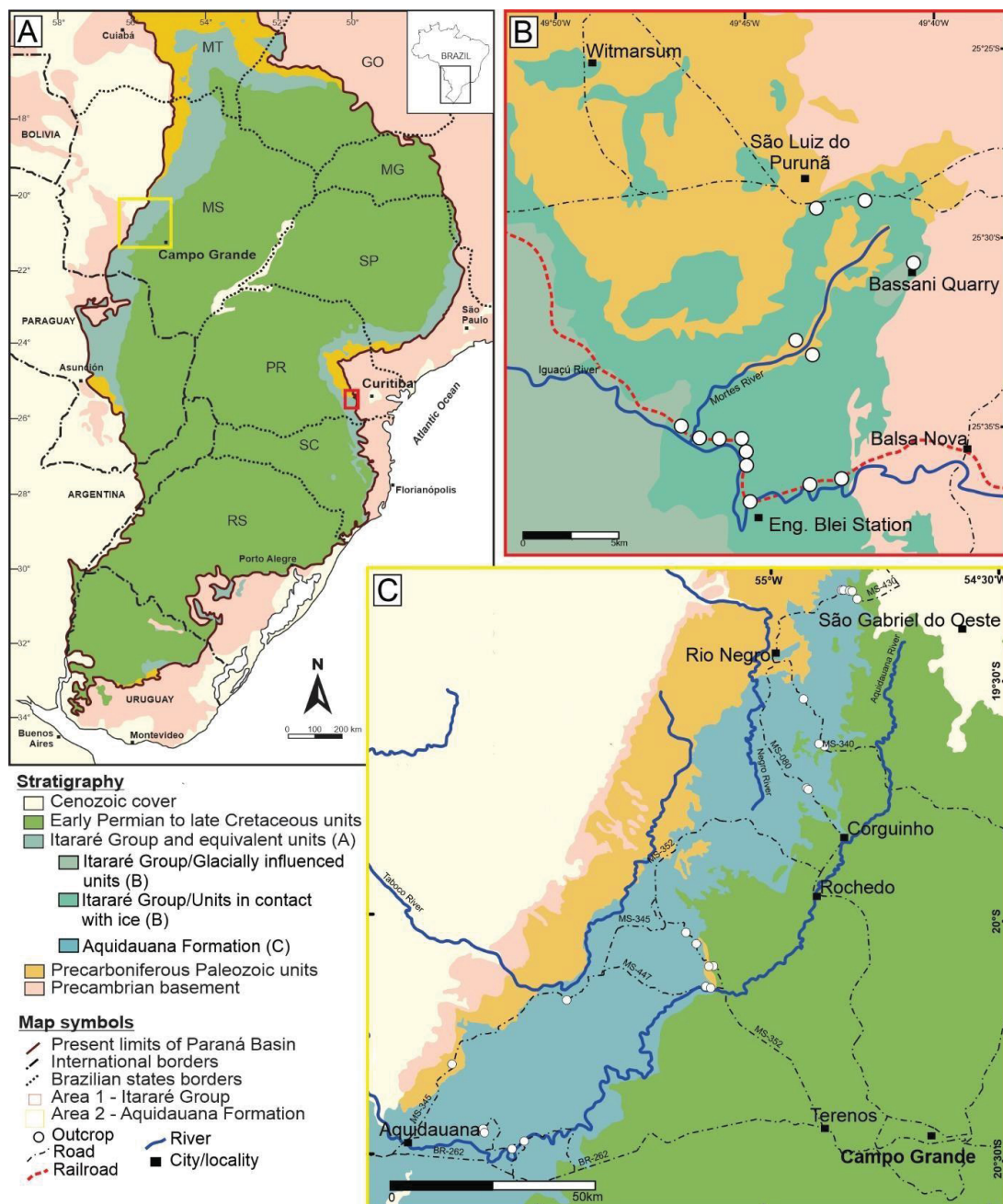


Fig. 5 Localization and simplified geology maps from study area. (A) Paraná Basin map with under and overlying units. Images B and C highlighted in red and yellow, respectively. (B) Detail of the studied area with described outcrops in Paraná state, next to Balsa Nova city. (C) Detail of the studied area with described outcrops in Mato Grosso do Sul state, northeast from Aquidauana city.

2.3 Methods

We described diamictites, sandstones, mudstones and rhythmites outcrops in Mato Grosso do Sul and Paraná states, from the Aquidauana Formation and Itararé Group respectively (fig. 05 B and C), adding up to 39 exposures. Facies and depositional settings have already been described by Gesicki et al. 1998 (Aquidauana Formation deposits) and Rosa et al. 2019 (Itararé Group deposits), where deformation caused by ice advance and mass movements was stated. We carried detailed description and measurements from deformation structures, such as folds, faults and shears, and collected oriented samples from deformed facies for thin sections manufacture. In total, we produced 40 thin sections parallel to the ice flow or mass flow direction in order to properly describe deformational structures and possible kinematic indicators. Once thin sections were done, we described microstructures, differentiating them in plastic, brittle, sediment mixing, pore water and post-depositional structures according to Van der Meer (1993) and also performing Phillips et al. (2011) micromorphological mapping.

2.4 Results

The laminated samples were taken from different stratigraphic levels in both lithological sets (fig. 6), representing deposits deformed by the direct action of the ice (sub or proglacial) and by gravity-driven mass flows.

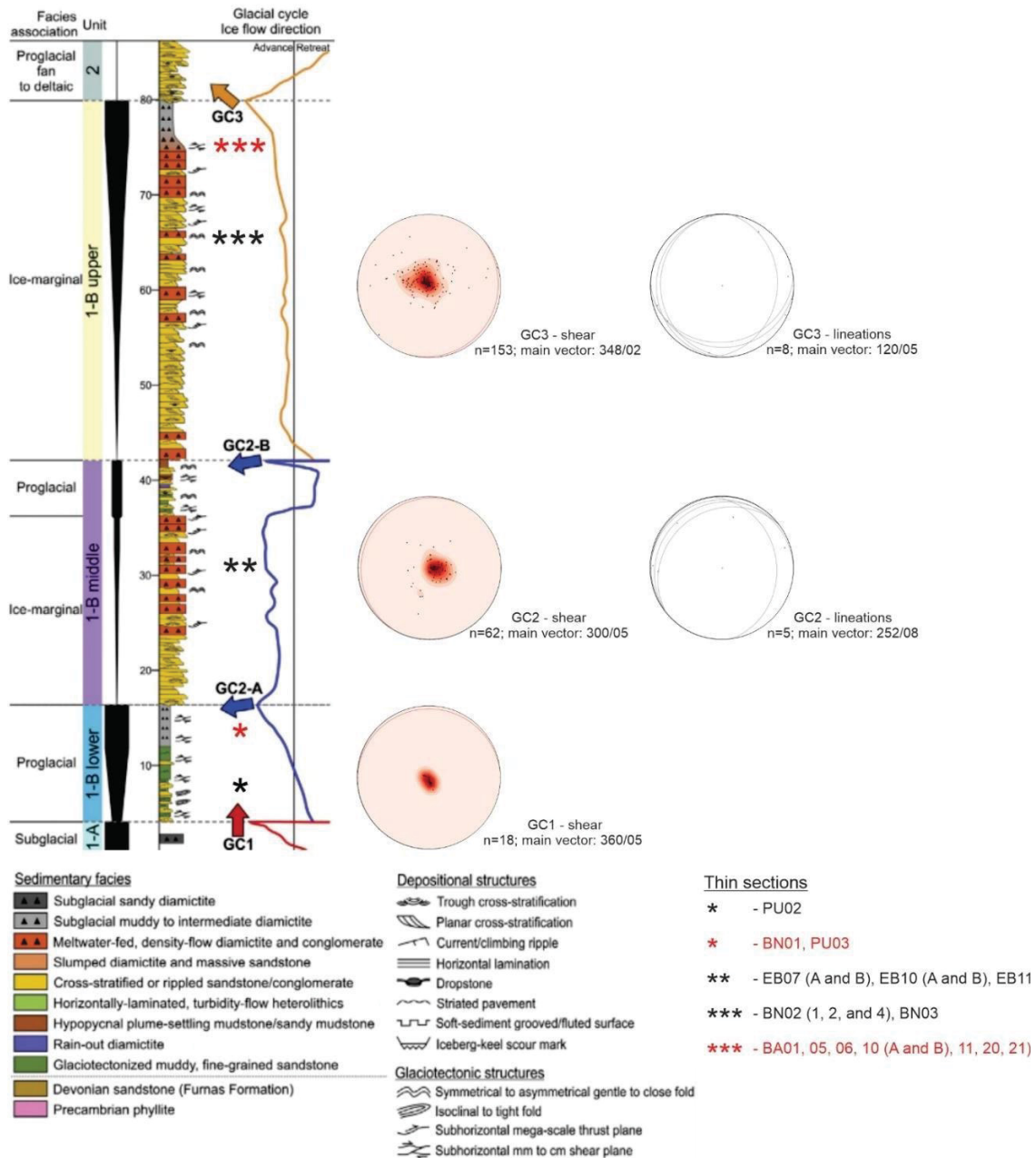


Fig. 6 Stratigraphic column of studied sucession from the Itararé Group (modified from Rosa et al. 2019), with stereograms referring to each glacial cycle and localization of thin sections.

2.4.1 Glacial-influenced deposits

2.4.1.1 Macroscopy

In the field, 233 shear plane measurements were obtained, separately interpreted according to the glacial cycles defined by Rosa et al. (2019) (fig. 06). In the first cycle, the planes with average direction N360/05 are generally parallel to subparallel to the accommodation. In the rocks of the second cycle, continuous and anastomosed subhorizontal shear planes were measured, with the average plane indicating a low dip to the NW and NE direction (N300/05). When observing the stereographic diagram referring to CG2, there is a small data dispersion, explained by the low diving angle and the waviness of the planes. The geometrical analysis of this unit's outcrops (asymmetry of folds and thrust faults) indicates transportation mainly towards the west, however there are slickenside measures that indicate movement to the southwest (N252/08). In the third cycle, thrust planes of average azimuth N180/10 and striations with a southwestward slope (N217/05) indicate transportation to the northeast. Decimetric horizons, which have undergone strong shearing in CG3, commonly isolate undisturbed portions, being formed by planes of millimeter-to-centimeter spacing, with an average dip of five degrees to the southeast (N120/05) (fig.5). In diamictites, sandstones and mudstones interpreted by Rosa et al. 2019, as glaciotectionized deposits, smooth and open folds up to 15 meters wide are also found (fig. 7A) along exposed sections of the Itararé Group.

Large thrusts faults and shear zones are described in the Bassani quarry in Balsa Nova, also found below and above the striated pavement (fig. 8A, B, C, D). The faults, in general, present irregular characteristics, with wavy planes that branch out and meet along the outcrop. Although uncommon, discreet striations can be found on some planes, especially on thrust fault planes. The difficulty in recognizing striations in the planes is largely due to the mainly sandy composition of the rocks (gravelly sandstones and sandy diamictites), whose rheology requires a greater effort to imprint and preserve the structures. Micro and mesoscopic drag folds in these planes also corroborate the reverse movement of the fault. Sometimes, morphologically similar structures of pressure shadows (although without recrystallization in the tails) are also observed around boulders, which can be used with a kinematic indicator (fig. 8F). Boudin-like structures are also observed in massive

sandstones in contact with stratified sandy diamictites in Gr. Itararé, indicating a possible rheological difference due to the greater presence of water (fig. 8E).

Smaller folds, with decametric to metric amplitude are also found just below the striated pavement in the Fm. Aquidauana (fig.7B, C), ranging from open to closed, with associated parasitic folds. These structures have a south-sloping axis, consistent with the ice movement described by Geisicki (1996). Folds on both margins of the Paraná Basin are also observed associated with thrust faults, such as drag folds, sheath folds and rootless folds (fig. 7D).

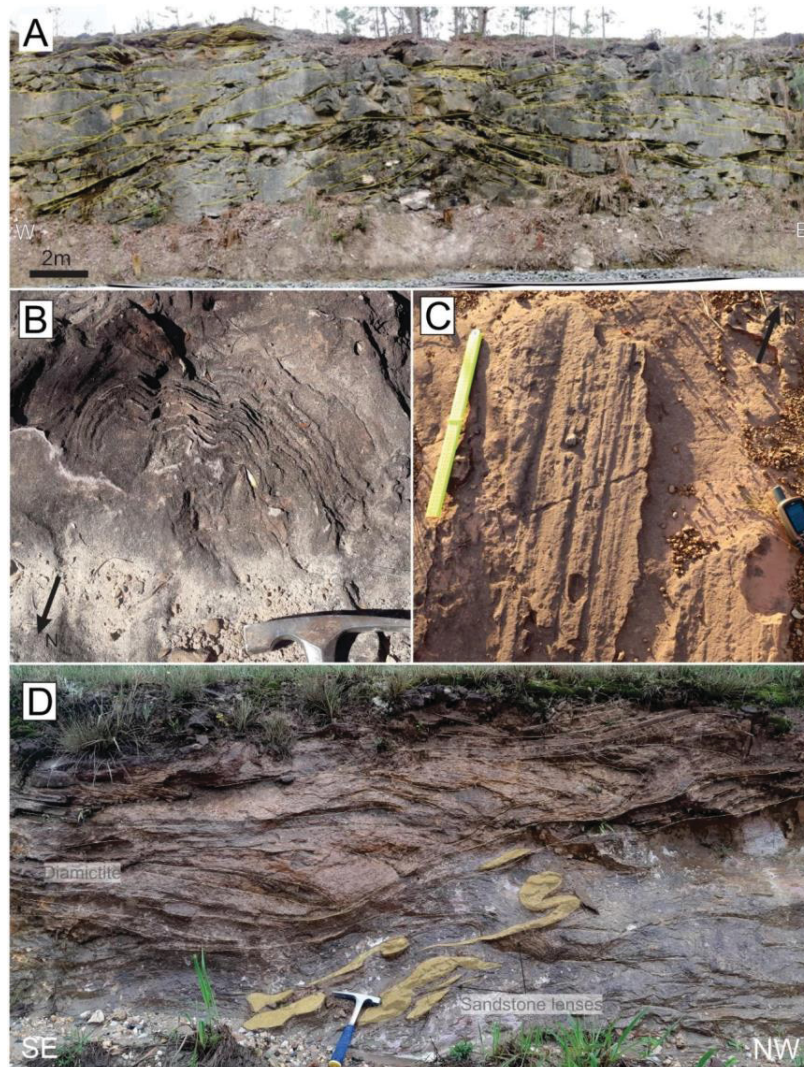


Fig. 7 Structures observed in glaciotectionized outcrops. (A) Open folds with metric amplitude and wave length in a diamictite rail road exposure from the Itararé Group. (B) Open folds with M, Z and S parasitic folds under striated pavement (C) from Aquidauana Formation. (D) Thrust with drag and rootless folds from Itararé Group outcrop.

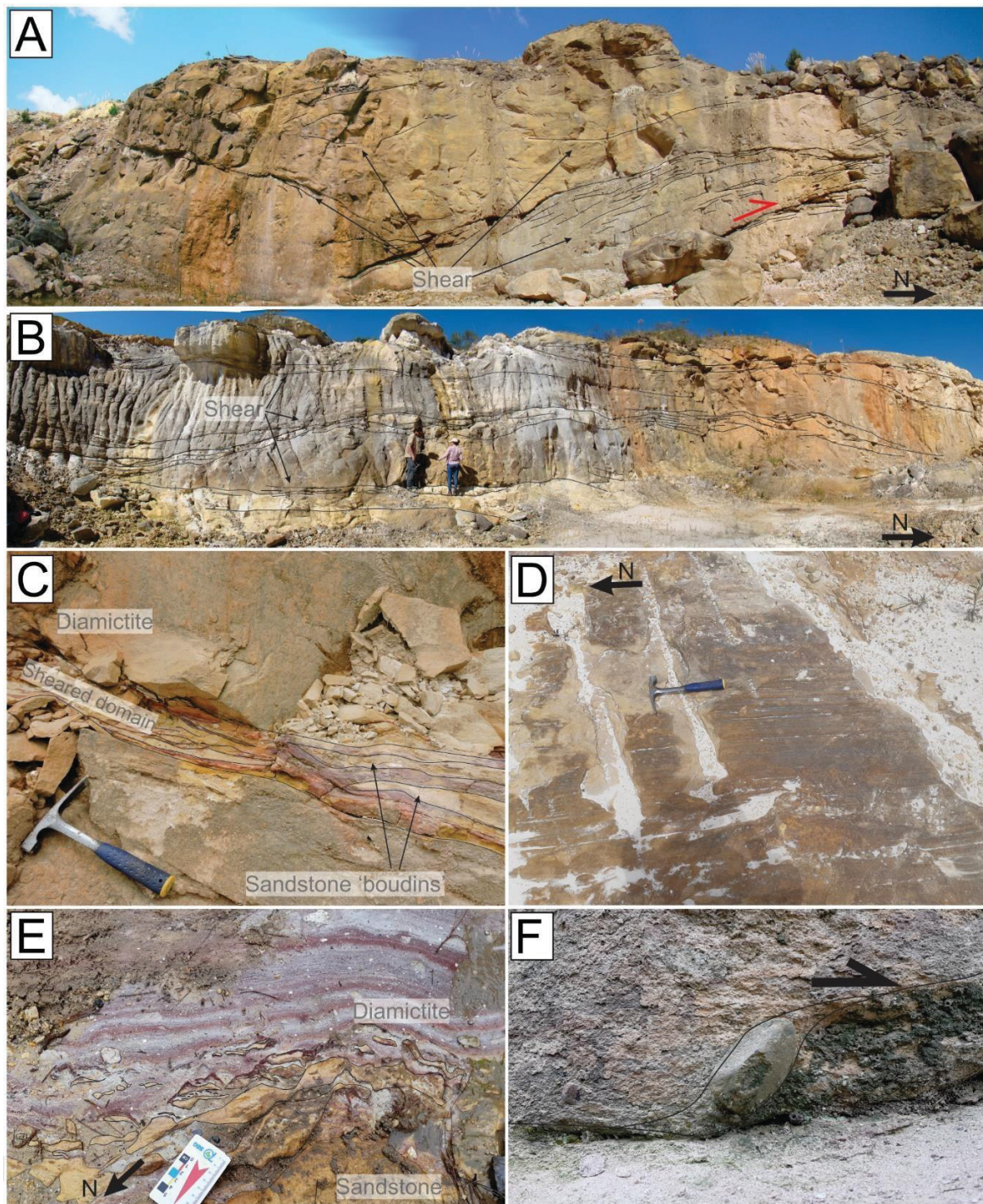


Fig. 8 Itaré Group exposures in Paraná state. (A) Thrust with narrow shear zones (transport northwards). (B) Wavy sheared horizons, notice onlap of layers on the sheared plane on the left portion of the photo. (C) Detail of the sheared portion. Boudinaged sand layers in muddy matrix. (D) Striated pavement in Bassani quarry. (E) Faulted coarse sand layers in contact with stratified diamictite. Arrow indicates north. (F) Rotated clast in sandy diamictite with shadow pressure indicating dextral movement.

In the shear zone, the structures' different branches form shear zones up to 60 centimeters thick (fig. 8C). Along these areas, cataclysmic rocks, which are generally more weathered, are described, with rare kinematic indicators, especially when they reach sand-rich layers. When at predominantly clayey levels, a more plastic deformation is observed, with boudinaged sand lenses and discrete shear planes that distort primary structures, such as laminations and stratifications.

2.4.1.2 Microscopy

From a microscopic point of view, several associations of characteristics are found, but none is considered as a diagnosis of the environment. Diamictites (both rich in mud and sand), poorly selected sandstones and mudstones were sampled, totaling 23 thin sections (some from the same sample).

Most *sensu strictu* thin sections of diamictites have characteristics formed by rotation, described in consensus in the literature as "ductile", the term "plastic" is employed in the present study due to the overlapping of definitions with classical structural geology, where a ductile deformation implies the presence of high temperatures. Features known as turbate structures are found in abundance, where smaller clasts form a circular or spiral alignment around larger clasts (fig. 9A, B). In poorly selected sandstones, these structures are not observed.

Still on the plastic deformation, folds of different styles can be found in thin sections, such as sheath, thrusts, closed and parasitic folds (fig. 9C, D). Folds are also observed associated with faults and boudin-like structures, such as drag folds close to the rupture of the layer (fig. 9E). These inflections are found in sandy and muddy samples, especially those that had the primary sedimentary band obliterated during deformation, but not completely homogenized.

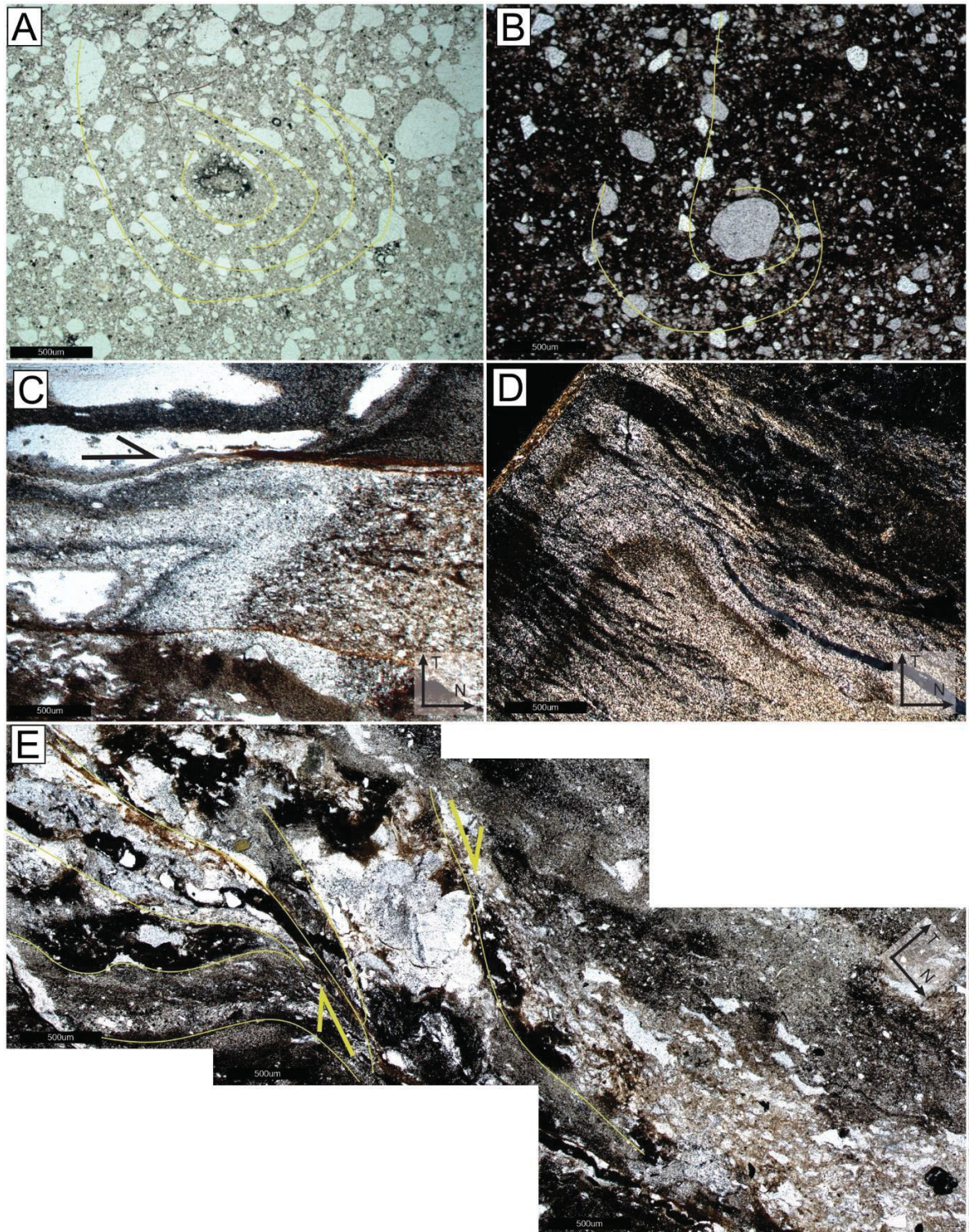


Fig. 9 Microstructures found in glacially deformed diamictites. Grain turbates in thin sections from the Itararé Group (A) sample BA11 and Aquidauana Formation (B) sample AQ15.3. Tight folds in diamictites from Paraná state (C and D), being C utilized as a dextral kinematic indicator (sample BA01). (E) Drag fold related to faults rupturing sand layer (sample BA01).

Microfolds, or crenulations, are deformed matrices, where there was first the intense development of plasmic fabrics and later the deformation of this fabric, which generates crenulations and even a second crenulation “foliation” (fig. 10A, B). In addition, crenulated detrital mica layers are observed in relatively well selected and compacted sandstones. The asymmetry of the crenulations suggests an oblique effort to bedding, discarding the possibility that the microfolds were generated only by compaction and diagenesis (fig. 10A, B).

These “foliations”, or plasmic fabrics, are subdivided into several categories depending on the development degree of the structure. Skelsepic, unistrial, banded plasmas and SC-like foliations are observed in the slides, defined by the orientation of fine minerals and phyllosilicates (fig. 10). When encountering rigid objects, such as clasts, the fabrics tend to circumvent them and generate “pressure shadows”, which are generally asymmetrical (fig. 10 E, F). In addition to "foliations" generated in plastic form, brittle fabrics (fracture cleavages) can be observed by obliquely cutting ($\sim 70^\circ$) plasmic fabrics developed in the first instance (fig. 10G). In addition to these 'pressure shadows', mica layers also provide kinematic indicators in both cases of dextral movement (fig. 10H).

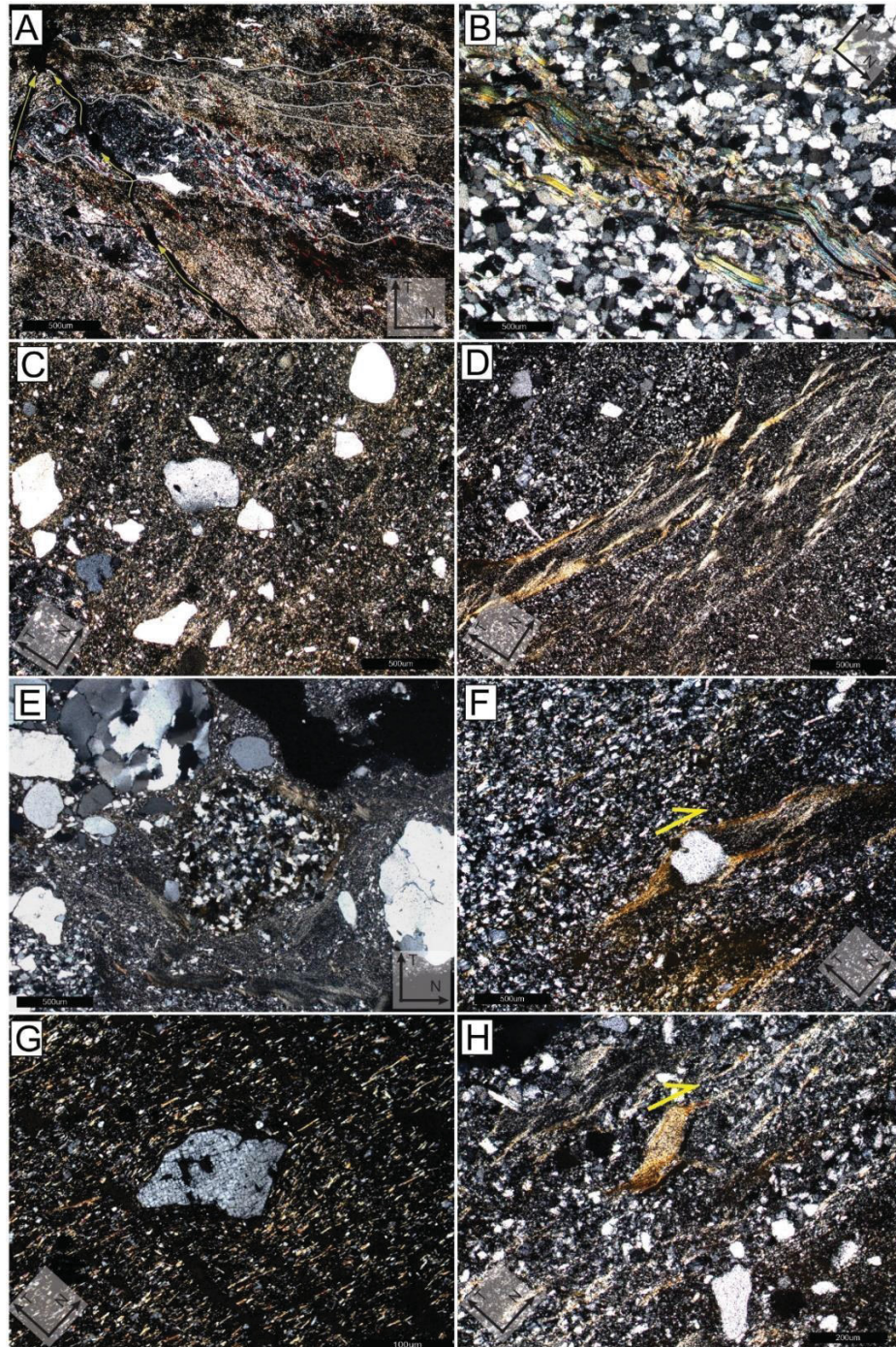


Fig. 10 Pseudo-foliations in glacially deformed samples. North to the right in all microphotographies. (A) Crenulated matrix from sample BA01 (S1, continuous black line) and crenulation cleavage (S2, black dashed line). Notice fluid scape structures (yellow arrows). (B) Crenulated detritic mica layers from sample BN03. (C) Skelsepic fabric in diamictites (BA10) and uniastrial plasmic fabric (BA06) (D). Shadow pressure around clasts from sample BA06 (E and F). Uniastrial plasmic fabric parallel to sample BN02-2 bedding with oblique cleavage fracture (G). Notice uniastrial fabric going around quartz grain. (H) Mica fish in sample BA06 indicating dextral movement.

With a brittle (or planar) behavior, shear zones are found in almost all observed slides, developing better in samples with higher clay content. Like those seen in outcrops, branches and fusions are observed in the thin sections, with planes marked with concentrations of clay and sometimes oxide (11D, E). The planes often bypass clasts that act as rigid objects, changing their orientation and/or generating 'pressure shadows' (Fig. 11A). Shear zones are also responsible for the fragmentation of clasts into fragments with high angulation and low sphericity (fig. 9E, 11B, C).

Mostly normal faults are observed in the thin sections as agents that break or obliterate sedimentary layers. Although they do not present well-formed planes, kinematics can be inferred from the displacement of the affected layers. Often, the faulting of less competent layers generate structures morphologically similar to boudins (boudins-like) (fig. 11F).

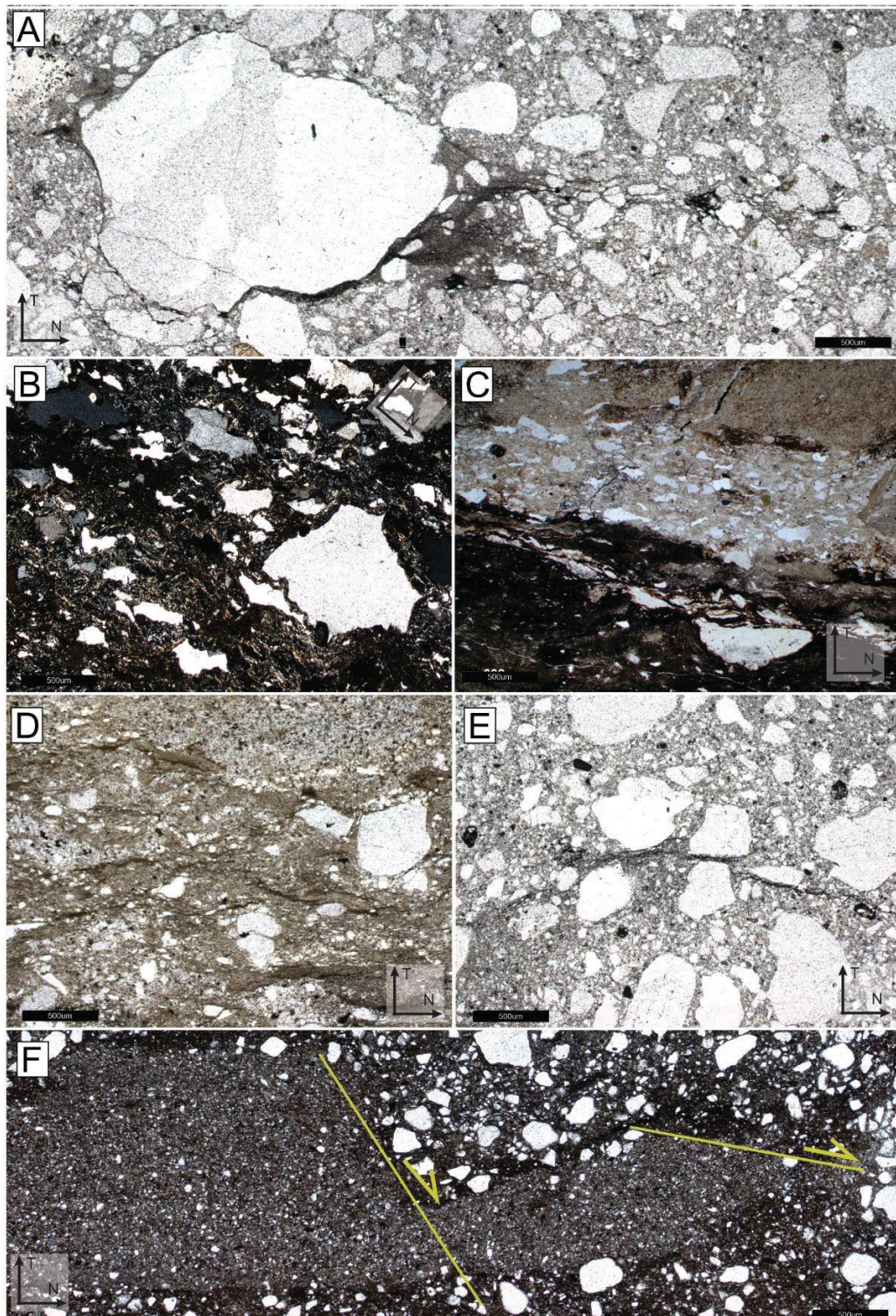


Fig. 11 Shearing features and brittle deformation in diamictites. (A) Sheared matrix forming shadow pressures around quartz grain (sample BA11). Sheared grains in sand layer from sample BA01 (B and C). Sheared matrix going around grains in samples BA06 (D) and AQ15.3 (E). (F) Very fine sand layer in diamictite with normal faults, sample AQ15.3.

Evidence of water leakage is not so common, most of the “paths” formed by water are very subtle, containing changes in grain orientation (towards the top), sometimes sand injections and layer disruption. Other features related to the presence of water are more common, such as the presence of multiple domains and grain coverage by clay and silt. Polygonal structures related to water leakage are rare.

In addition to deformational structures, there was some evidence of the influence of diagenesis on the rocks. Concave-convex and sutured contacts are common in sandstones (Fig. 12A), and stylolites are found in at least two samples, with two different orientations in one of them (Fig. 12B). Corroded grains, stains caused by percolation of oxide-rich fluids, differential compaction, as well as overgrowth of quartz around grains and partial dissolution of cement are also observed (fig. 12C, D, E).

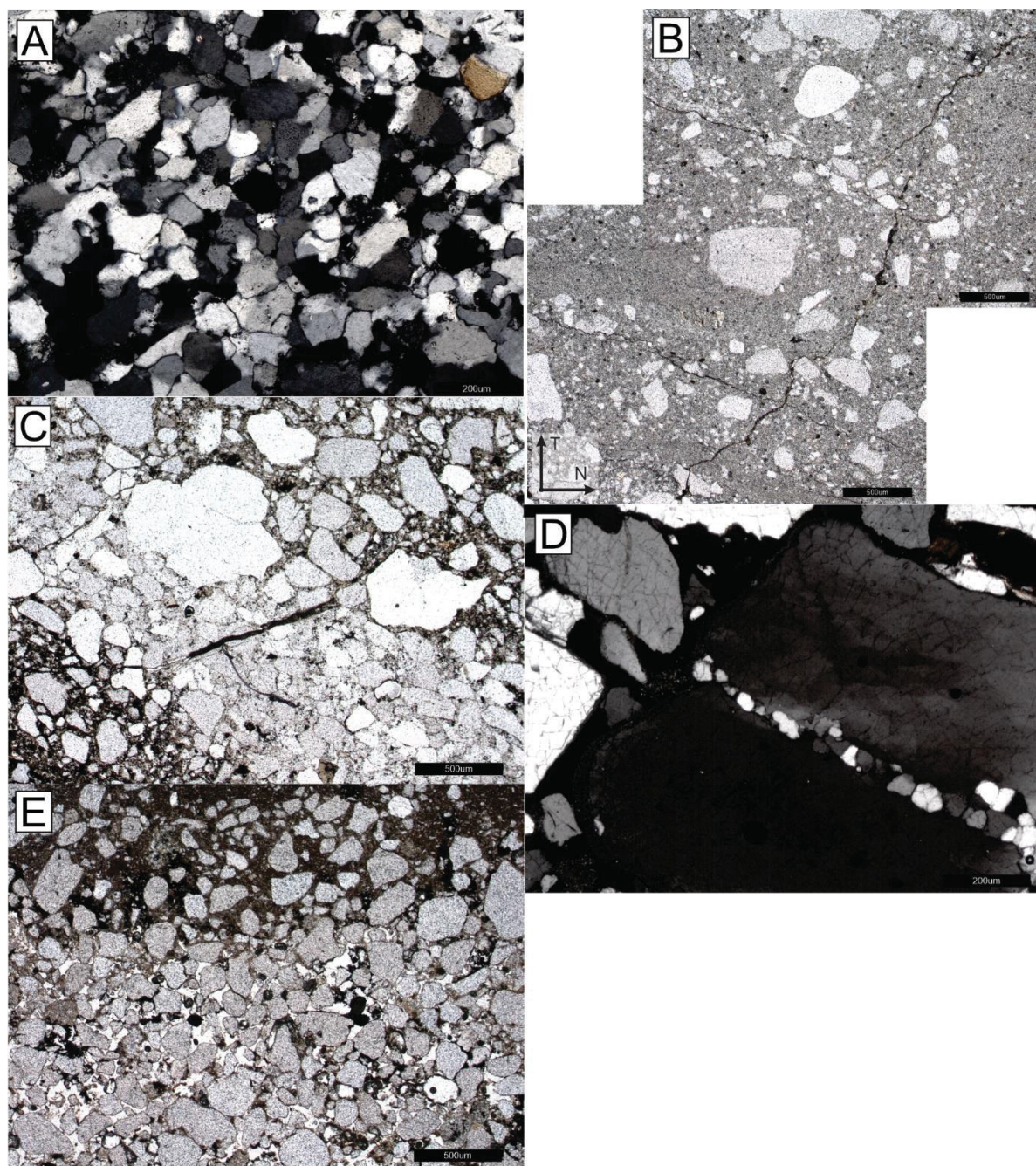


Fig. 12 Diagenetic features in glacially deformed rocks. (A) Concavo-convex and sutured grain contacts in quartz grains in sample BN03. (B) Stylolites in two different directions, with 90° angle between them – sample BA11. (C) Differential compaction in layers with and without matrix in sample PU02. (D) Cement partially dissolved in sample AQ15.3.

2.4.1.3 Linear fabrics (lineation)

To map the alignment of clasts and define trends, 12 thin sections, six from the same spot, were analyzed. Despite the work of Phillips et al. (2011) having coined the term “foliation” to describe the plots formed by the alignment of clasts, we chose to use the term “lineation” in this work to distinguish these structures from the plasmic fabrics described above. Thus, we have the term “lineation” used to describe linear fabrics.

The sections made from a striated pavement (AQ15.1, .2, .3, .4, .5, .6) are coherent with each other, with only one that differs from the rest. Thin sections AQ15.1, .2, .3 (fig. 13A, B, C), .4 and .5 have a strong horizontal orientation of clasts (S3), with a plunging pattern to the southeast (L1) at angles varying from 45° and 15° in relation to the horizontal, due to the wavy character of the fabric. When cut, an incipient lineation with dip to NE (L2) presents high variation in their angles, being also associated with the wavy character of the fabric. Finally, a discrete vertical orientation indicates the presence of water leakage (fig. 14). If we look between the alignments of three or more thin sections, we see most of the clasts are aligned with dikes to SE, especially with angles around 20° (fig. 13D). The previously predominant horizontal orientation appears discretely, indicating that the formation of the L3 lineation was incipient, generating discontinuous geometries.

Contrastingly, the AQ15.6 thin sections presents a great dispersion of the clast orientations, with subvertical, subhorizontal linear fabrics and dipping for both NE and SE. This dispersion is explained by the sampling having been carried out in the hinge zone of a fold, with the influence of several axial planes in the orientation of the clasts.

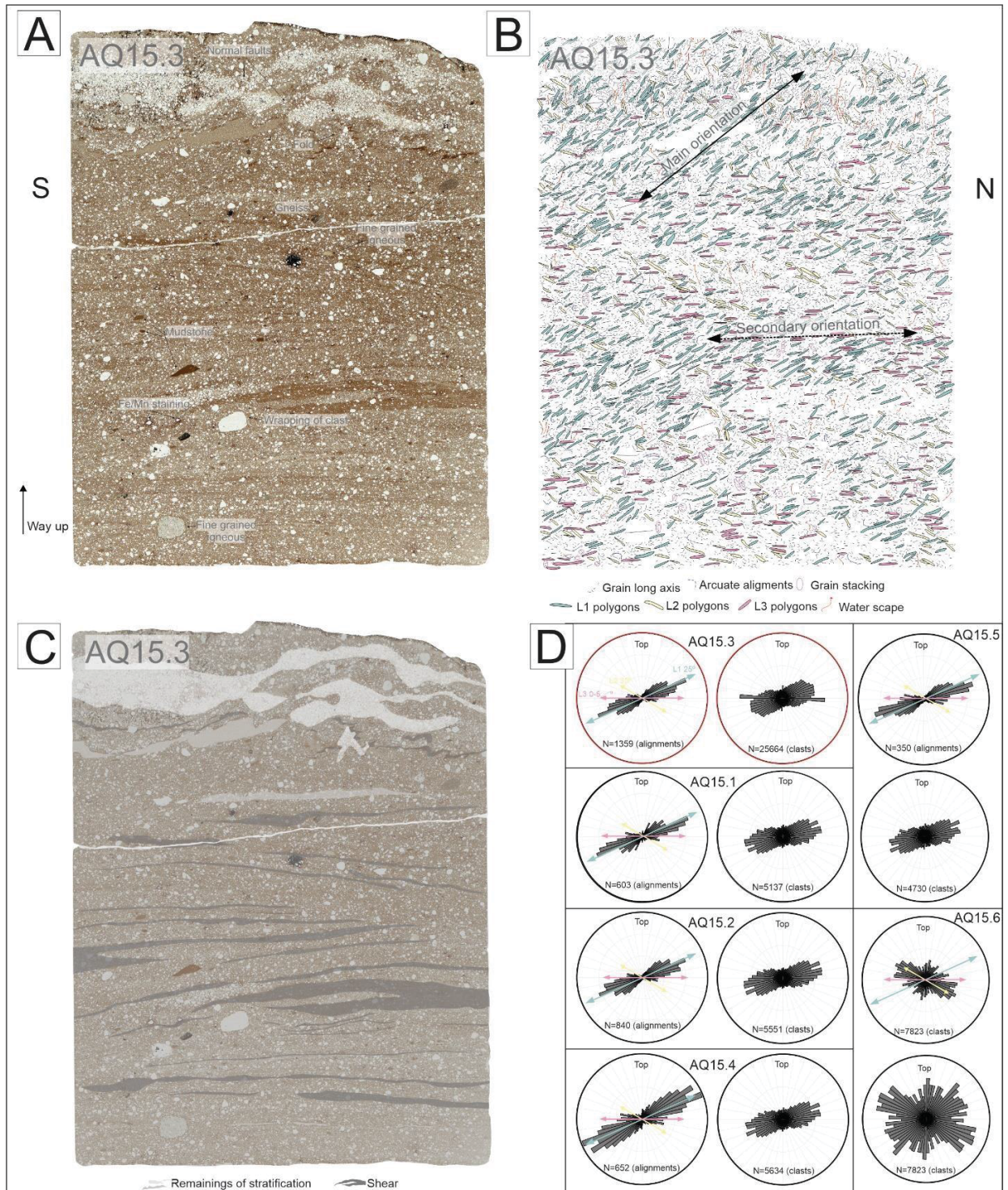


Fig. 13 Linear trends map from sample AQ15. (A) High resolution scan from thin section in parallel nicols, highlighting clasts main compositions and structures found. (B) Referred polygons to the different mapped lineations, as well as shears, fluid scape structures and clasts bigger axis orientation. (C) Reliquiar layering and shear structures. (D) Rose diagrams from the six thin sections from sample AQ15.

With similar fabrics, the BA06 sample represents a stratified diamictite, where different structures are formed depending on the material (fig. 14A). In the sand-rich portions, granules and pebbles, oriented clasts are observed, while in the muddier portions there are several shear planes and the generation of plasmic fabrics. These planes are discontinuous, spaced, and irregular, with low dips for SE and NE, a variation consistent with their wavy features (fig. 14 B, C). When comparing the shear plane and foliation orientation with the orientation of clasts, a difference is noted, both regarding the angle in relation to the horizontal and the direction of dips. Lone clasts are divided into three strong orientations, from the most eminent to the most incipient: subhorizontal, dipping for NE and dipping for SE. The lineations formed by more or three aligned clasts indicate strong orientation with dipping towards NE, followed by a lineation falling to SE. Once again, there is a decrease in the influence of subhorizontal clasts (fig. 14D).

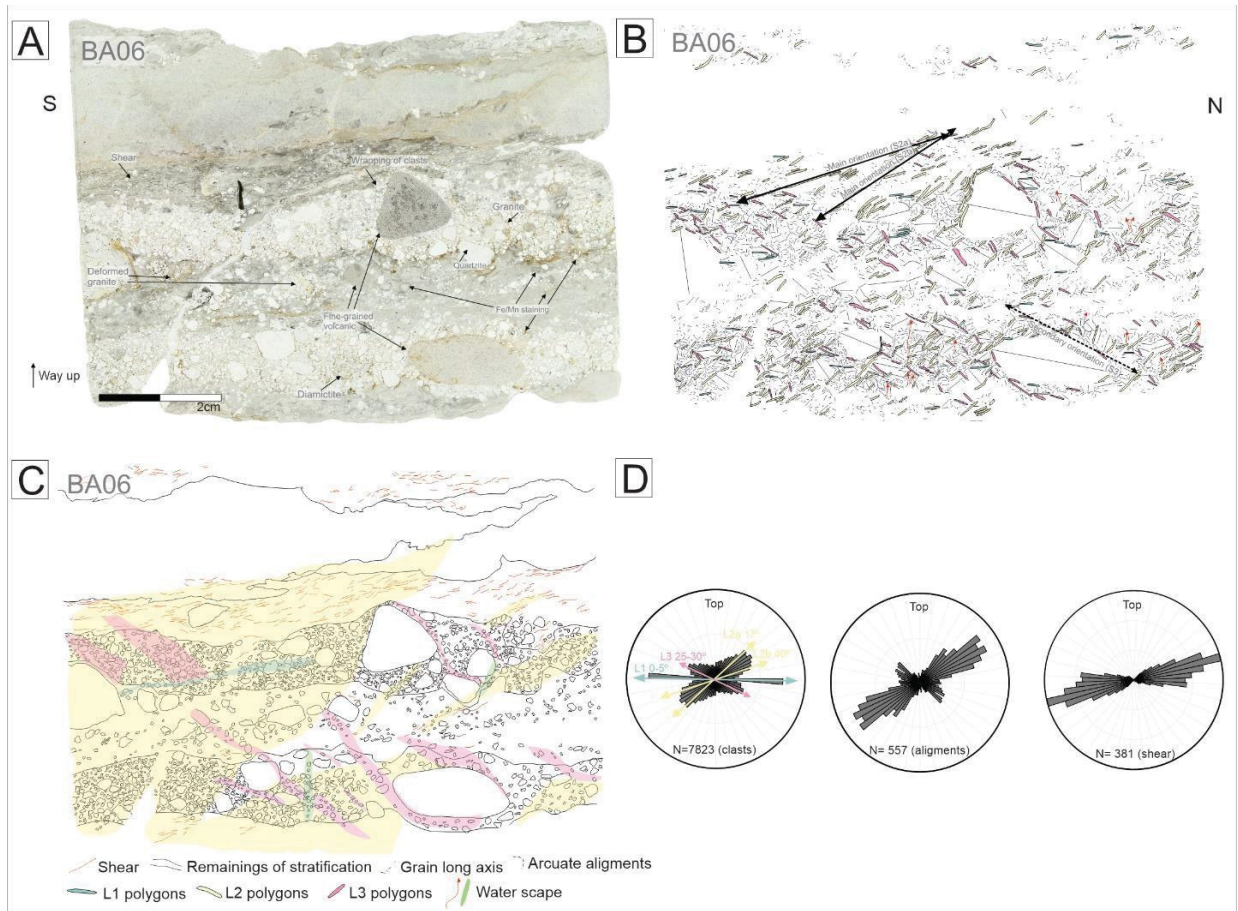


Fig. 14 Linear trends map from sample BA06. (A) High resolution scan from thin section in parallel nicols, highlighting clasts main compositions and structures found. (B) Referred polygons to the different mapped lineations, as well as shears, fluid scape structures and clasts bigger axis orientation. (C) Main lineation trends. (D) Rose diagrams of mapped clasts, clasts alignments and shears.

With a high dispersion in the orientation of clasts, the BA10 sample (fig. 15A) partially maintains this spreading when evaluating the preferred direction of the lineations (fig. 15C). Even so, three linear fabrics can be individualized. The cutoff relation between them, however, is not clear due to their great spacing and discontinuity, preventing the definition of a hierarchy. When comparing the lineation data with the shear data, obtained through micas oriented in plasmic fabrics, these three directions mentioned above are observed, two of them with a morphology similar to a SC pair (fig. 15B) and the third subhorizontal with wavy and discontinuous planes.



Fig. 15 - Linear trends map from sample BA10. High resolution scan from thin section in parallel (A) and crossed nicols (B), highlighting clasts main compositions and structures found. (C) Rose diagrams of mapped clasts, clasts alignments and shears.

Another thin section that has consistency between the axes of the clasts and the lineations between them is the EB10. With a strong general trend of diving for SE, it is possible to individualize, observing the rosette diagram, three trends with dives of $\sim 15^\circ$, $\sim 40^\circ$ and $\sim 60^\circ$. Subvertical trends are also observed, with a lower average NE dip. Hierarchically, we would first have the formation of the lines with the highest dive for SE, with consequent “evolution” for the two lowest dive trends. The orientation with opposite dive is formed soon afterwards, with discontinuous and irregular planes cutting the other plots. Finally, fluid leakage generates subvertical trends.

Patterns with intense data dispersion are observed in samples BN02-4 and PU02. Similar to each other, even with the dispersion, the general trend of diving towards SE is remarkable, with subordinate lines to SE and subvertical. Just like the samples described earlier, the orientation of individual clasts loses expression when analyzing the orientation between three or more aligned clasts.

Although not oriented, only with the top indication, the BA11 thin section (fig. 16A) presents coherence between the data, especially when comparing the individual clasts with the trends of clasts aligned with each other. Preferred horizontal orientations are observed with a low diving angle, with data spreading and decreasing the frequency towards higher dives. If we also compare the shear data, it is possible to observe horizontal and subhorizontal dives as the most expressive, followed by dives up to 30° , without the vertical spread observed in the clasts and lineations (fig. 16B, C).

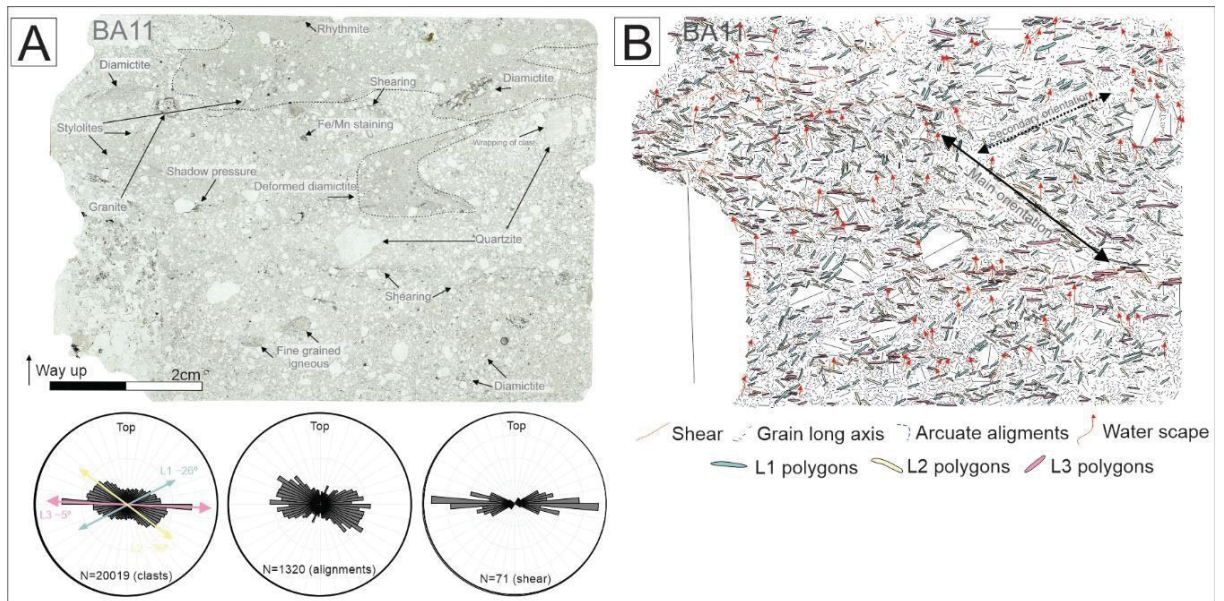


Fig. 16 Linear trends map from sample BA11. (A) High resolution scan from thin section in parallel nicols, highlighting clasts main compositions and structures found. (B) Reffered polygons to the different mapped lineations, as well as shears, fluid scape structures and clasts bigger axis orientation.

2.4.2 Mass-transport deposits

2.4.2.1 Macroscopy

In the field, mass movements of the Itararé Group are identified by abrupt contacts, often erosive, with the adjacent and underlying rocks, sometimes forming sets of mass movements with more than one event. Commonly of muddy matrix and poor in clasts, it is possible to observe block-in-matrix rocks in the middle of a more homogeneous matrix. Inside the blocks, it is often possible to recognize preserved sedimentary structures, while the edge of the block may have striations related to its deformation. These blocks may have other deformational structures, such as *sensu strictu* boudins, folds, and faults (with associated boudins-like). Normal and reverse faults occur in mass movements, the normal ones being from the Itararé Group with an average dip of 30° for SE and those from Fm. Aquidauana with higher values, exceeding 60° , for E-SE. In turn, reverse faults with average dives of 25° indicate transport to N-NW in the Aquidauana Formation. As for the matrix, it is common to observe shear planes near the block, in addition to intra and extrabasinal clasts. Mixing, or homogenizing features of the matrix and blocks are also described.

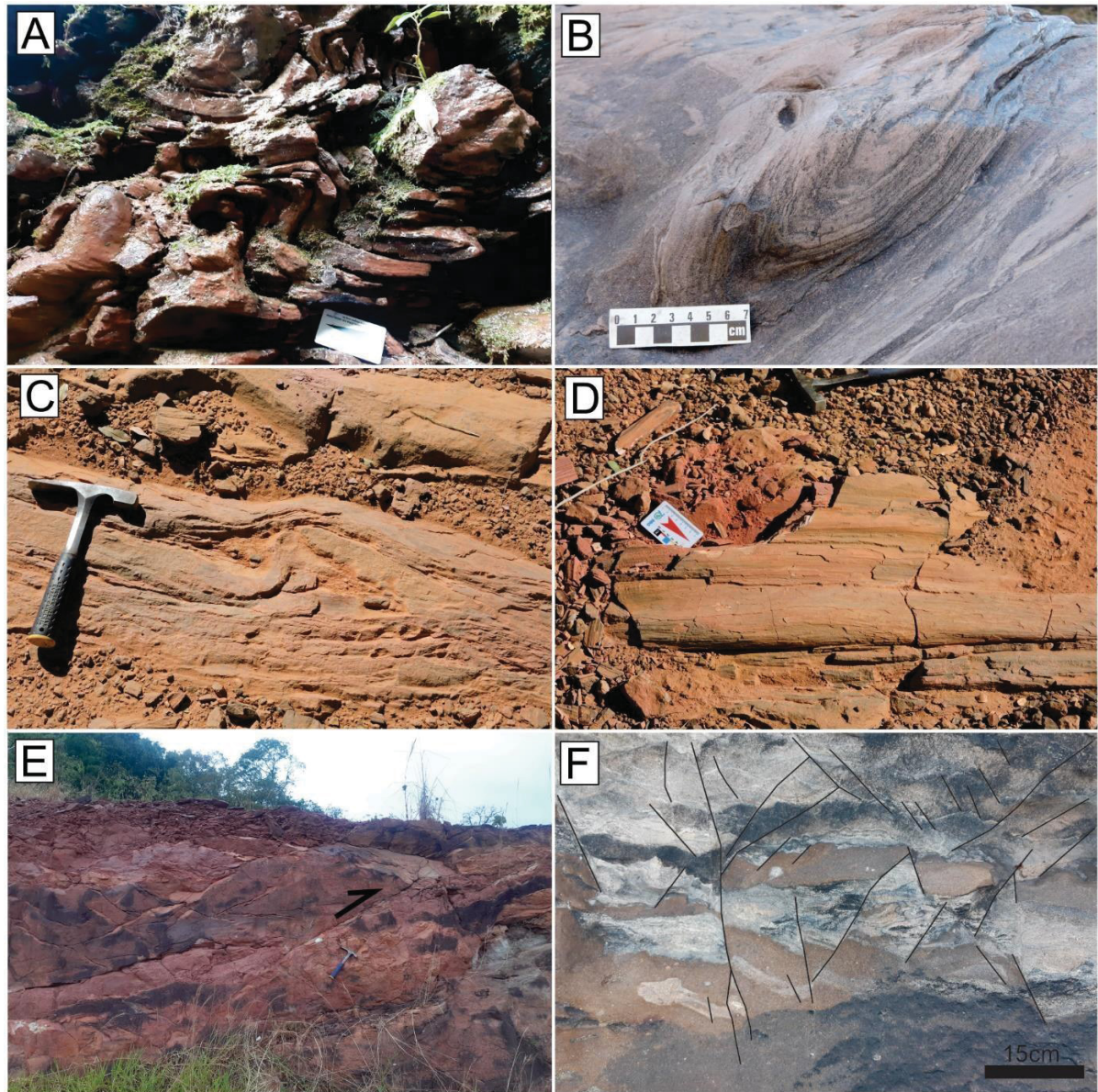


Fig. 17 Deformational structures from mass transport deposits from the Aquidauana Formation. Folds with different limb openings: tight in section view (A), recumbent (B) and tight in plan view (C) associated to recumbent folds with intersection lineation (D). Hammer indicates north. (E) Thrust faults in clast poor diamictites from Aquidauana Formation. (F) Layered clast poor diamictite with reverse and normal faults. Notice that more intensively faulted areas become more homogenized.

In addition to the "evolved" mass movements, both in the Itararé Group and in the Aquidauana Formation, deformed deposits with a lower degree of homogenization are described, with faults (normal, reverse and thrust and, fig. 17E, F), folds of different styles (fig. 17 A, B, C, 18C), lineations (fig. 17D), shear blocks and boudin-like features. In the outcrop, it is possible to describe large shear zones by cutting the exposure and isolating large undisturbed portions (fig. 17A). These planes generate two concentrations of poles with great spreading among themselves, referring mainly to the two largest expressions of planes diving to the northwest and others to the southeast, respectively (fig. 17A).

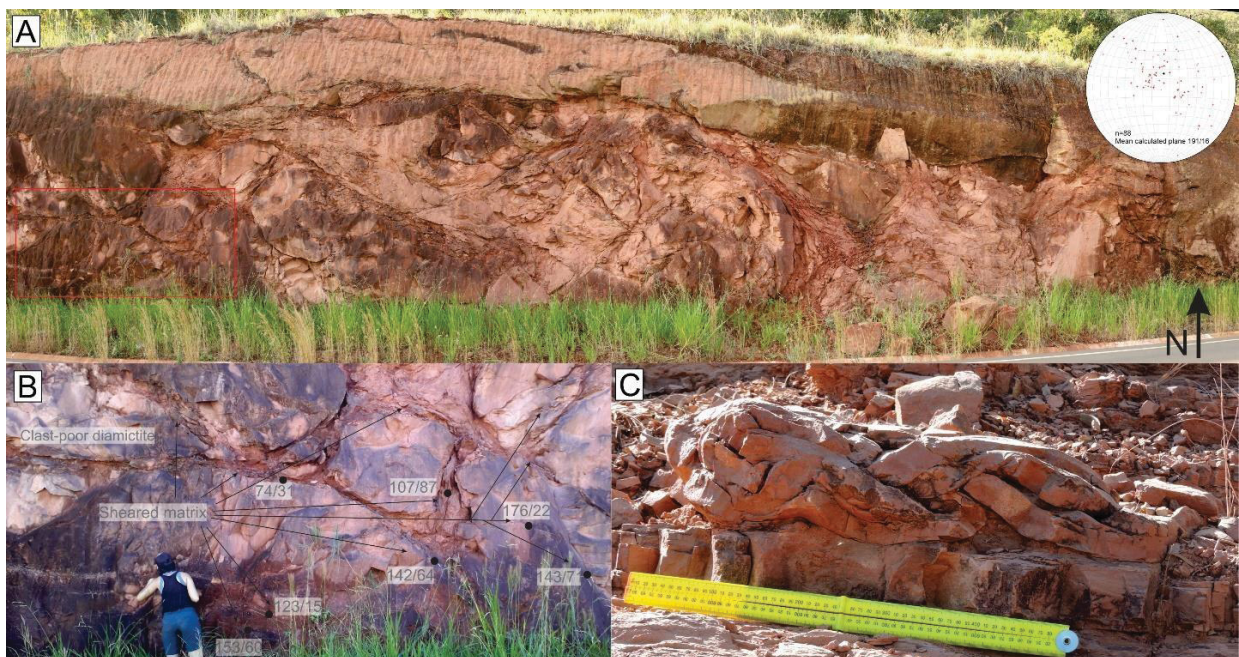


Fig. 18 Mass transport deposits with shear planes (A) that goes around apparently undeformed blocks (B). (C) Intra-stratal folds from Aquidauana Formation.

Despite the large expression of muddy rocks in the outcrop, samples of coarser granulation (poorly selected sandstones and sandy diamictites) were selected for lamination, due to the applicability of the techniques used being based on larger granulometries.

2.4.2.2 Microscopy

Four thin sections from mass movements were prepared, aiming to characterize folds, faults, and unrecognizable structures in a hand specimen. From these, diverse

structures were observed related to both rotation and planar shear processes, in addition to fluid leakage.

When analyzing faulted sandstones, it is possible to observe the development of sand smears along the fault planes, sometimes with a slight grain comminution. It is also possible to note that, within the smears, the sand grains tend to change their orientation, becoming parallel to the fault planes (fig. 19A). In these sandstones, shear features can also be found, in addition to boudin-like geometries of faulted layers, drag folds and pseudo-pressure shadows (fig. 19D).

In a thin section made perpendicular to the axial plane of a sheath fold, it was possible to observe parasitic folds, broken slides, shear features, and small normal and reverse faults that interrupt the sedimentary banding (fig. 19B). Because it is a fine stratified sandstone, with very fine sand and silt intertwined, on rare occasions it is possible to observe rotation features, such as grain turbates (fig. 19C). Despite presenting prone characteristics, the development of plasmic fabrics in the thinnest thin sections of the rock was not observed.

Contrastingly, poorly selected sandstones with a silt-clay matrix (diamictites) exhibit a larger and more frequent range of structures. The AQ20 sample has grain turbates, pressure shadows, shear features and lineations formed by grain alignment, in addition to grain stacking (fig. 20), related to both rotation and planar deformation processes. In terms of plasmic fabrics, only discrete unistrial fabrics were characterized in the clay-rich portions of the sample.

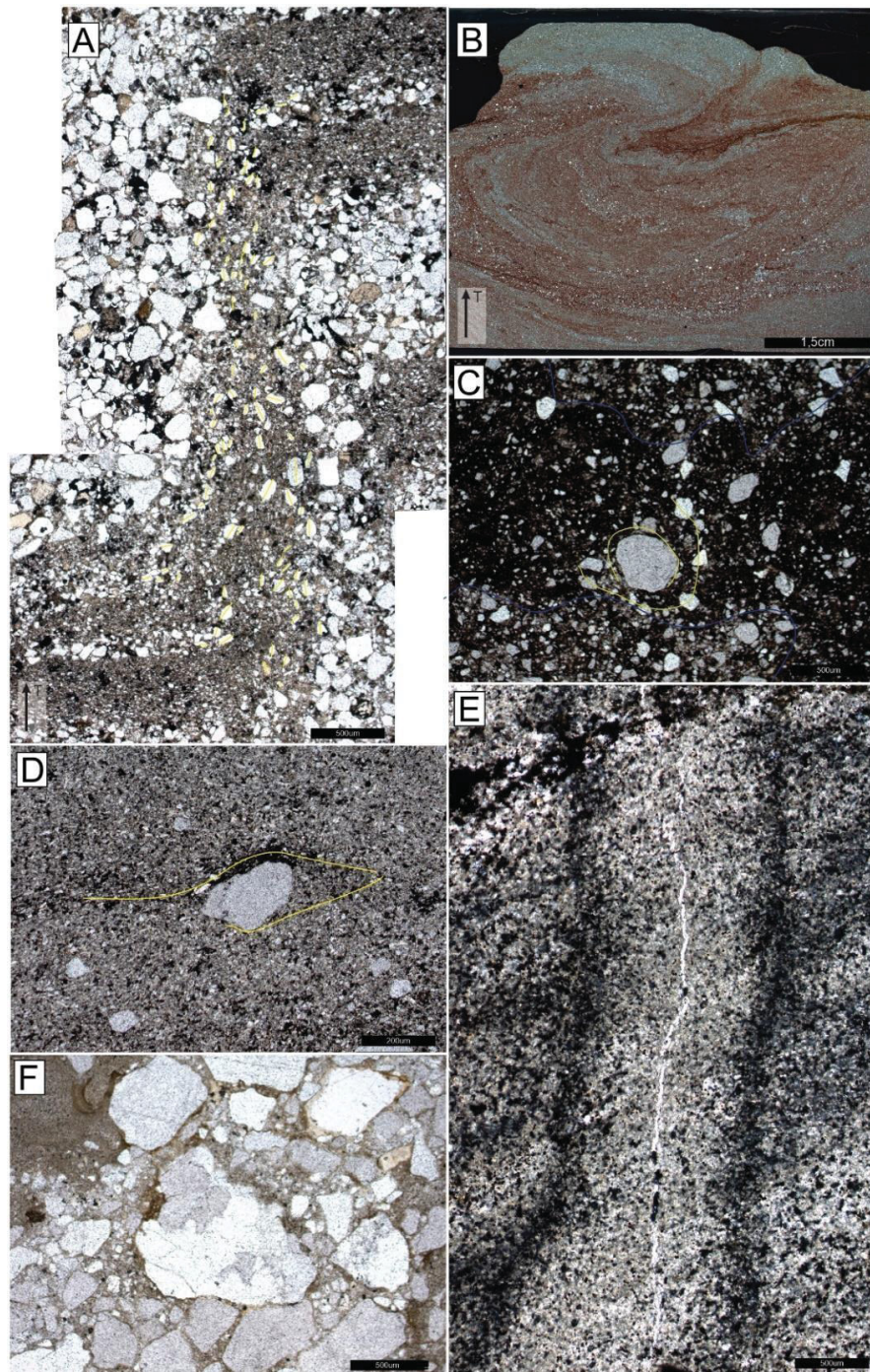


Fig. 19 Microstructures described in thin sections from mass transport deposits. (A) Sand smearing in fault planes from poorly sorted stratified sandstone. Notice change in clast orientation, that become parallel to the normal fault (sample AQ17). (B) Crossed nicols scan of folded rock (recumbent fold), with fault nearly rupturing the superior limb. Sample AQ06. (C) Grain turbate (yellow) and multiple domains (blue) in diamictite. Sample AQ06. (D) Discrete pseudo- shadow pressure (yellow) surrounding quartz grain. Sample PU03. (E) Structure related to fluid scape in sample PU03. (F) Clay coating in polycrystalline quartz grain. Sample AQ20.

Structures known as fluid leaks are also described, especially “paths” made by water during the escape, multiple domains and silt and clay coatings (fig. 19).

2.4.2.3 Linear fabrics (lineation)

Only the mapping of the AQ20 sample was carried out, due to the greater granulometry.

Analyzing together the preferred directions of the clasts, lineations and plasmic fabrics foliations, it is possible to notice a great coherence between the data. Individually, the clasts have preferred dives close to horizontal, with symmetrical drop dispersion to the south and north (fig. 20). Trends with higher diving to the north can be subordinately identified by cutting the previous lines, as well as an orientation formed last, with high dives to the south, coming close to the vertical.

However, the clasts aligned with each other have better individualized populations of trends, with a low dip both south and north. In a similar way, the shear features occur, but with higher slopes than those observed in the alignments and a more defined population with high diving to the south.

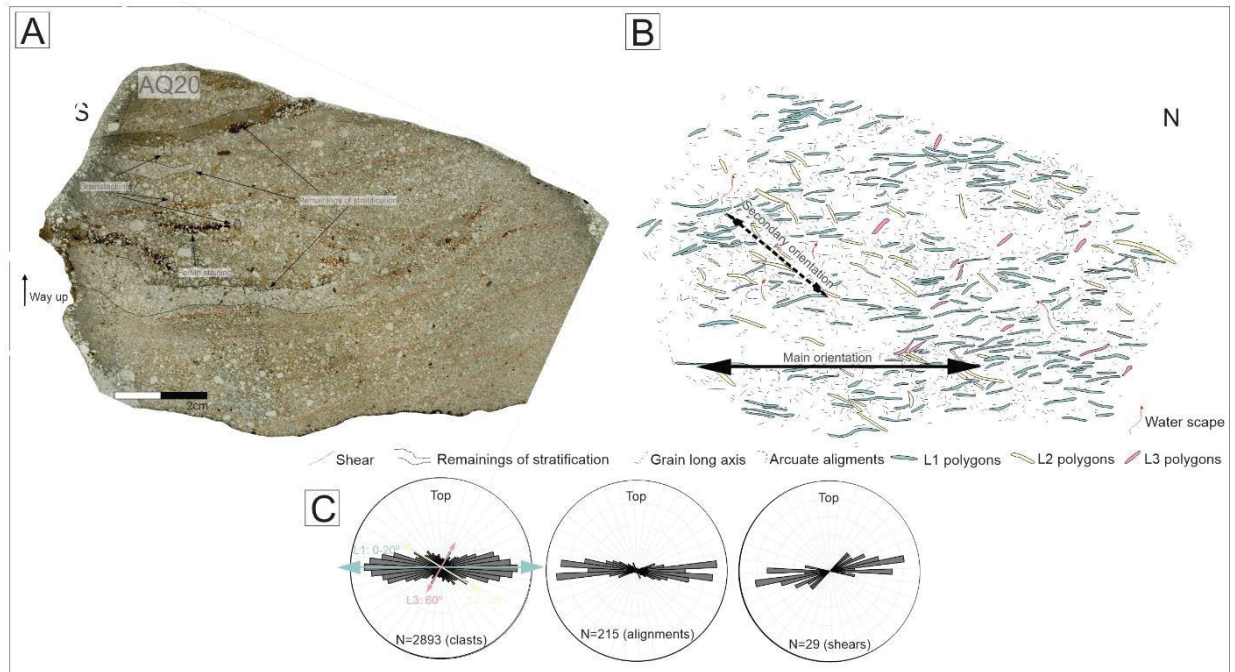


Fig. 20 Linear trends map from sample AQ20. (A) High resolution scan from thin section in parallel nicols, highlighting clasts main compositions and structures found. (B) Referred polygons to the different mapped lineations, as well as shears, fluid scape structures and clasts bigger axis orientation. (C) Rose diagrams of mapped clasts, clasts alignments and shears.

Similar to the mapping of clasts, rosettes were made from the delimitation of flaws in hand specimens (fig. 21A, C), which proved to be easier to identify than in thin sections. On slide, however, it is possible to observe the comminution of the grains within damage zones, as well as their orientation parallel to the fault planes, as in the case of sample AQ17B (fig. 21C). It is also possible to observe that the color difference that defines the banding and aids to highlight the displacement generated by the faults is caused by oxides filling spaces in layers that, apparently, were more porous, which was also detected by observing hand specimens under an electronic magnifying glass.

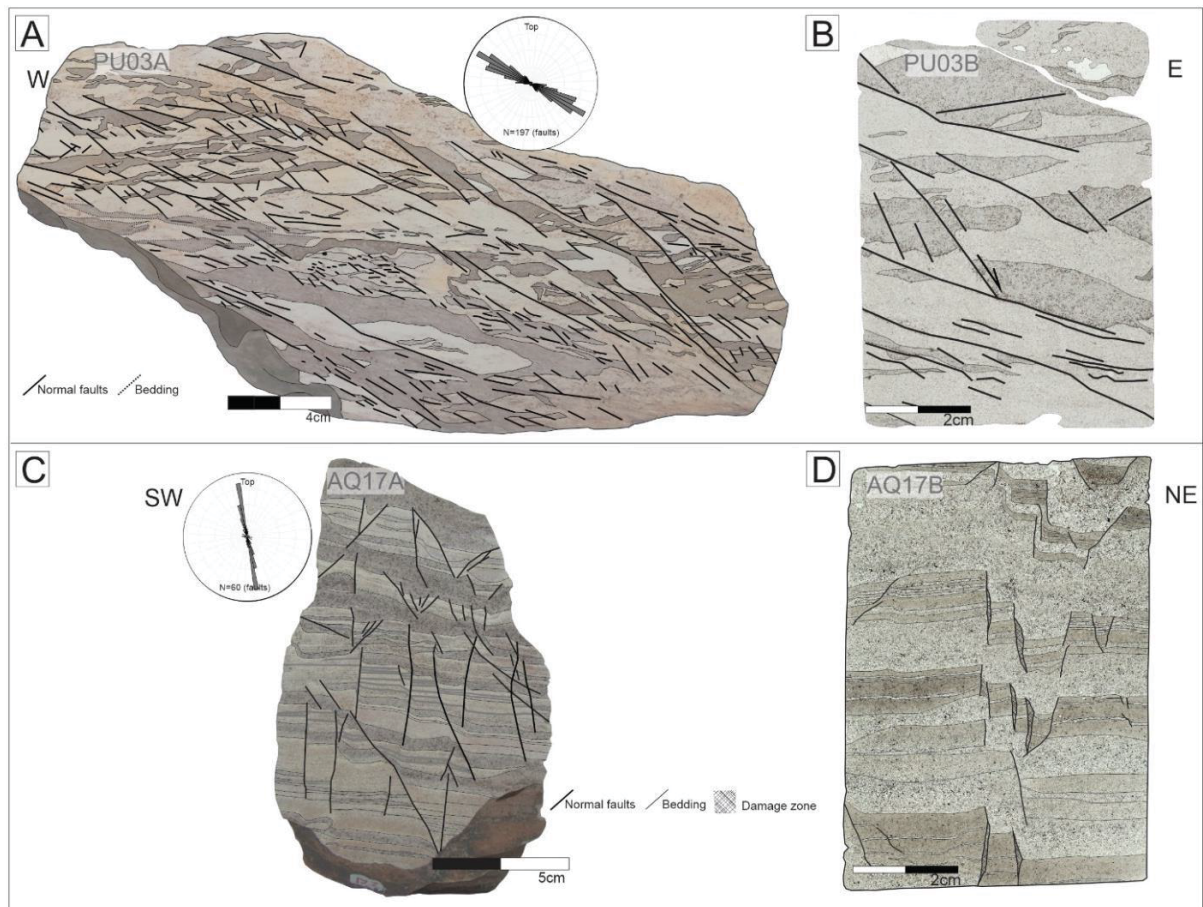


Fig. 21 (A) Sample PU03A with mapped faults and layering. (B) High resolution scan from thin section (PU03B) in parallel nicols, with mapped faults and layering. (C) Sample AQ17A with mapped faults and layering. (D) High resolution scan from thin section (AQ17B) in parallel nicols, with mapped faults and layering.

2.5 Discussion

2.5.1 Development and preservation of microstructures and linear trends in Paleozoic rocks

It is evident that the development of structures in sediments by glaciotectionics and gravitational movements is not restricted to macroscopic features. Altogether, 21 different microstructures have been described (table 1), among brittle, plastic, fluid leakage structures, depositional powders, and others, indicating a high degree of preservation of these structures.

Table 2 – Described microstructures in thin sections from Itararé Group and Aquidauana Formation.

Sample Number	Def. Setting	Plastic					Brittle			Sed. Mixing		Pore Water			Plastic Fabric					Post depositional				
		Grain Turbates	Boudins/Lenses	Shadow pressure	Shears	Grain alignments	Folding/crenulation	Normal Faults	Reverse/Thrust Faults	Sheared grains	Intraclasts	Multiple Domains	Water Escape	Polygonal structures	Clay and silt coating	Skeletal	Uniaxial	Banded plasma	SC like foliation	Stylolites	Conc.-Convex Contacts	Sutured contacts	Quartz overgrowth	Fe/Mn staining
AQ21	Ice Keel	x							x									x		x				x
AQ22	Intrastrata																							x
AQ06.2	MTD	x		x		x		x	x					x										x
AQ17	MTD					x		x																x
AQ20	MTD	x		x	x	x				x	x	x	x	x			x							x
PU03	MTD			x	x			x				x												x
BA05	Proglacial	x					x			x	x	x		x							x			
BA06	Proglacial			x	x	x		x																
EB07 (A and B)	Proglacial	x			x												x							x
BN02-1	Sub/Proglacial	x		x	x		x				x	x					x	x	x					
BN02-2	Sub/Proglacial				x		x																	
BN02-4	Sub/Proglacial					x					x													
BN03	Sub/Proglacial						x																	
AQ15.1	Subglacial	x		x	x	x		x				x												x
AQ15.2	Subglacial	x		x	x	x		x				x												x
AQ15.3	Subglacial			x	x	x				x		x												x
AQ15.4	Subglacial	x			x	x						x												x
AQ15.5	Subglacial	x			x	x						x												x
AQ15.6	Subglacial	x			x	x						x												x
BA01	Subglacial			x	x	x		x		x		x						x	x					x
BA10	Subglacial	x		x	x	x				x														x
BA11	Subglacial			x	x																			x
BA20	Subglacial	x		x	x	x																		x
BA21	Subglacial																							x
TR201	Subglacial	x		x	x	x																		x
BN01	Subglacial	x																						x
PU02	Subglacial			x	x	x																		x
EB10 (A and B)	Subglacial	x		x	x	x																		x

Pervasive deformation observed both in diamictites as in sandstones and mudstones is evidenced by the presence of rotational structures, clast alignments, shear features and “pressure shadows” (Baroni & Fasano 2006). Such a deformational style is also evidenced by the presence of cataclastic rocks, generating angular and irregular components that may be the result of high strain on grain contact or high pore pressure (Hiemstra & van der Meer 1997).

Furthermore, plasmic fabrics are visible in most samples, especially unistrial ones, being absent in rocks with a lower percentage of clay. In some cases, as in the case of samples BN02 and BN03, these fabrics can be observed in the hand specimens, from the orientation of the micaceous minerals that are concentrated in well-defined planes. The concentration and reorientation of micas in planes is commonly caused by pressure dissolution in response to the stress imposed on the material (Fossen, 2010).

The mapping of clasts to obtain linear fabrics proposed by Phillips et al. (2011) was also shown to be possible for Paleozoic diamictites, with microfabrics formed by the passive rotation of skeleton grains (Carr & Rose 2003; Carr & Goddard 2007).

2.5.2 Influence of diagenesis

Structures related to post depositional processes are represented mainly by secondary features related to the impregnation of oxides and dissolution and reprecipitation of silica, generating concave-convex and sutured contacts between the grains and quartz overgrowth.

Alsop et al. (2017) point out the need for caution when interpreting Soft-Sediment Deformation Structures (SSDS) in the geological record, as compaction and diagenesis can cause changes and enhancements in the structures generated in unconsolidated sediments. The authors also point out the uncertainties that may arise during the distinction between Soft-Sediment Deformation (SSD) and Hard-rock Deformation (HRD).

According to Farrell & Eaton (1988), the two main processes responsible for creating or modifying SSD fabrics are liquefaction and compaction, while liquefaction causes the grains to pass through particulate streams, changing thin sections and layers, compaction is created from burial of the material, transmitting pure deformation with vertical shortening and enhancement of subhorizontal fabrics created during the SSD. Maltman (1981) also suggests that, with the

increase in the depth of burial, diagenesis can “halt” primary fabrics related to the accommodation or grain compaction. The growth of new mineral phases during diagenesis can then be controlled by the guidance of a pre-existing sedimentary fabric. However, the enhancement of subhorizontal linear fabrics is not observed in the thin sections whose mapping of clasts was carried out, where oblique components are much more prominent. The emergence of new mineral phases oriented according to the pre-existing fabrics is observed in some samples with advanced development of plasmic fabrics. This is the case of samples BN02, BN03, BA06, BA10 A and B, where micaceous minerals defining foliations (or stretching lineations, in the case of the last two samples mentioned) are visible even to the naked eye, possibly due to the late growth of micas and/or originally detrital clay minerals.

Maltman (1981) suggests that the presence of interstitial water reduces intergranular friction, facilitating the rotation of the grains to create parallel flat stratifications of compaction, occurring early in the sediment trajectory, in the first few meters of burial. This statement is questioned by Elliot & Williams (1988), who noted that these deformational plots are absent from testimonies in modern sediments that are less than 100 meters deep in relation to the ocean floor. Thus, there is an ambiguity regarding the necessary depth of burial for the generation of compaction stratification.

As compaction is applied uniformly not only to deformed sediments, but also to undeformed sediments, structures generated from it should be found in both cases. However, this is not what is observed in the study area, with non-deformed intervals having only sutured contacts and cement dissolution in some cases, without the formation of compacting foliations (considered by authors such as Fossen 2010, as a non-deformational feature). Normal faults measured in rocks of the Itararé Group showed smaller angles than expected for this type of fault (60° , Fossen 2010), with average dips of 30° . Although this may be an indication that there was a flattening due to diagenesis, smaller dipping angles are more expected in unconsolidated sediments than in rocks, due to the charging factor. The critical condition in which the material is fractured can be calculated from the internal coefficient of friction, which for rocks is a constant (0.47-0.7, 0.6 being the most used value), but for sediments the critical angle of repose is used, in this case $\sim 30^\circ$ for sand (Fossen 2010). At Fm. Aquidauana flaws are found with dips equal to or even higher than 60° , with subtle comminution of the grains along the fault planes,

indicating some degree of lithification at the moment of deformation. Push faults found in both Gr. Itararé and Fm. Aquidauana with dipping values as expected (10 to 40°, Fossen 2010) corroborate the hypothesis that, despite the diagenesis, the angular relations between structures maintained the expected values.

2.5.3 Are the fabrics described in thin sections correlated on a regional scale?

Analyzing together the rosette diagrams of the clasts mapped to rocks of the Itararé Group, we can see some similarities between the defined fabrics (fig.22). In samples BA11, BA10 and EB10, the first and most evident fabric to be formed (L1) has a moderate dip to the southeast. When cut, there is a second lineation (L2) also with moderate dips, however towards NE. These two microfabrics define a set of “down-ice and up-ice dipping Riedel shears” (Phillips et al. 2018) (L1 - type P shear and L2 - type R shear). In these thin sections it is observed that the last trend to be formed is the sub-horizontal one (L3 - Y-type shear), which can be a diagenetic product, since there are many horizontal clasts, but these do not form an expressive fabric. This geometric and hierarchical consistency between the data indicates the deformation occurred under similar conditions of deformational regime (Phillips et al. 2011), consistent with the interpretation suggested by Rosa et al. 2019 as subglacial-deformed.

The BA06 sample clearly differs from the rest, with L3A and B as the main fabric, despite the fact that it has dipping angles similar to the L1 observed in the other samples, the cut ratio with the other plots shows that this was the last to be formed. This different hierarchical relationship, with the type P shear being the last to be formed, may better reflect either different pore pressure conditions and quantity of water than the samples aforementioned, or else be a reflection of the context in which the sediment was deformed, in the proglacial case.

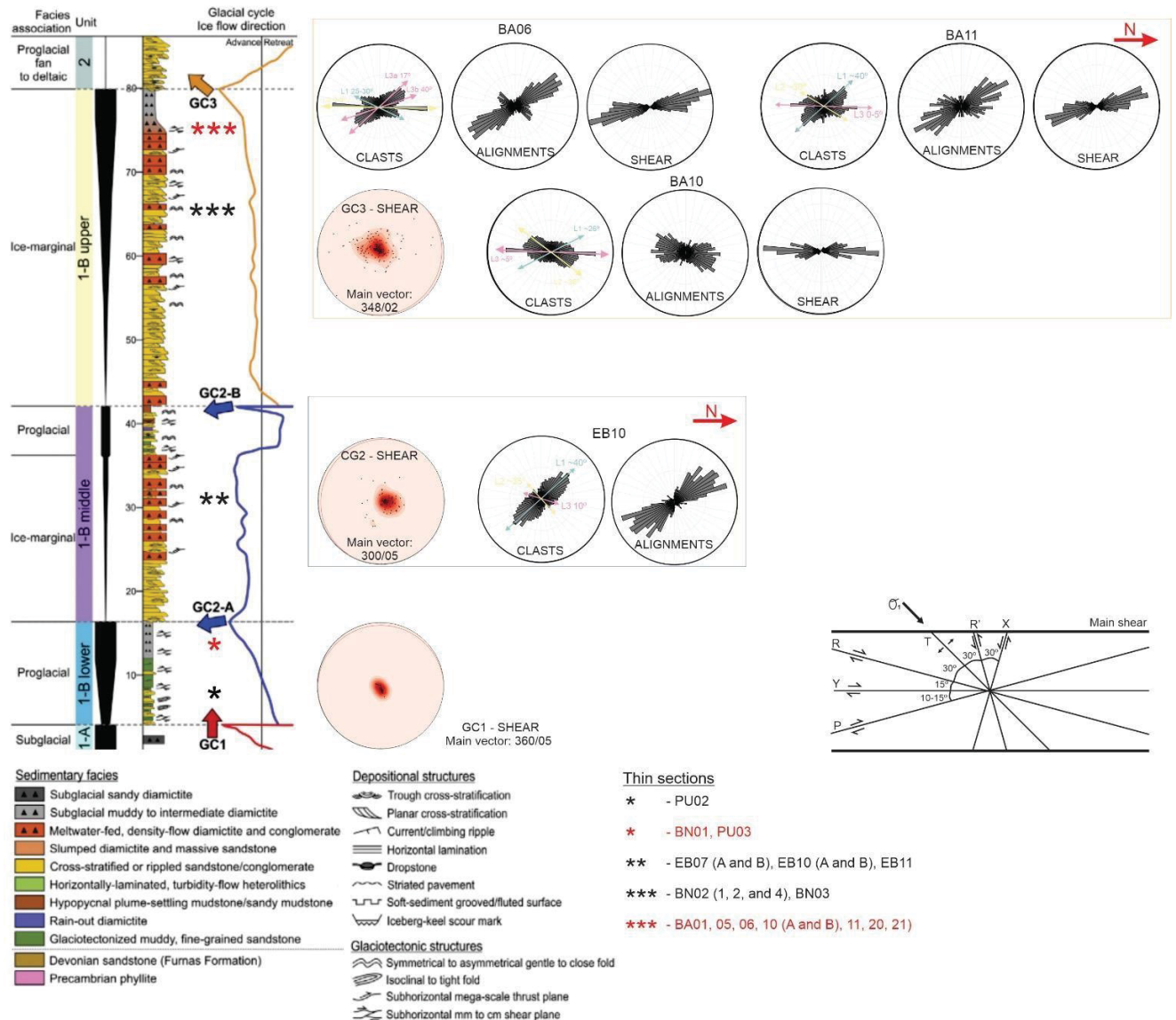


Fig. 22 Stratigraphic column from Itararé Group (modified from Rosa et al. 2019) and rose diagrams of mapped clasts and shear structures.

It is worth mentioning that as the orientations between clasts are formed by their rotation, it is often the case that they encounter larger clasts that act as rigid objects, forcing trends to circumvent them, changing the dip angle, leading to greater variations than one would expect from tectonic deformations. Another factor that should be considered when analyzing trends is that the effort applied to the sample is neither uniform nor constant over long periods of time, with factors intrinsic to the sample being sometimes more relevant in forming trends, such as water content, pressure of fluid and clay percentage.

2.4.1 Structures in glacial (glaciotectonite) and gravitational (MTDs) deformed sediments

The use of micromorphological aspects in the differentiation of diamictites deposited in different depositional environments was the focus of several published articles (van der Meer 1987; Lachniet et al. 1999, 2001; Carr et al. 2000; Carr 2001; Menzies & Zaniewski 20003; Carr et al. 2006, Phillips et al. 2006; Menzies et al. 2006; Reinardy & Lukas 2009; Kilfeather et al. 2010). These studies recognize that a large part of the structures found in glaciotectonites can also be observed in MTDs (faults, folds, boudins, rotation structures, etc.), indicating that the process responsible for the deformation of these sediments is the same, so the structures are not diagnoses of a particular environment (Phillips 2006). This aspect is observed in the samples studied in the present research, where, by observing only the microstructures whose classification was proposed by van der Meer (1993), they are indistinguishable. However, the pattern of linear fabrics formed *en mass* vs. mass movements is noteworthy in glaciotectonites, with the lineations formed in the AQ20 sample having many more horizontal trends than in any other studied section. This characteristic may be an indication of strong basal shear stress, which is the common transport mechanism for mass movements, indicating that the deformation was concomitant with the placement of the deposit, and not generated by subsequent stress (Phillips 2006).

Another aspect that is notable is the abundance of normal faults in gravitationally deformed deposits in relation to those deformed under a glacial context. These faults can be synthetic or antithetical to the flow movement, for which it is recommended the use of other kinematic indicators to determine it (Rodrigues et al. 2020). These structures are described by Rodrigues et al. (2020) as one of the first features to be developed during the deformation of MTD, usually in the proximal portions, leading to the gradual homogenization of the deposit.

2.6 Conclusion

The multiscale analysis of deformation in sediments generated by glaciotectonism and mass movements of rocks, deposited during the Late Paleozoic Ice Age in the Paraná Basin, using structural field data and those obtained from microscopic analysis techniques traditionally used in recent deposits proved to be highly efficient:

- With the identification of more than 20 different microstructures, the classification proposed by van der Meer 1993 is also applicable to rocks in the geological record, as well as the mapping of clasts proposed by Phillips et al. 2011.
- Despite generating some features, such as partial dissolution of cement, concave-convex contacts to sutures and stylolites, diagenesis is not a process that significantly erases or even obliterates the registration of SSDS. As the intensity of diagenesis is conditioned by the amount of matrix in the rocks, being more intense in those with less or no matrix, the analyzed diamictites suffered little influence.
- There is a high degree of agreement between the data of linear fabrics between deformed rocks on the same process, being different when compared with deformed material under distinct conditions. However, it is important to consider that in the deformation of sediments, intrinsic factors such as pore pressure and water saturation exercise great control in the structures generated.
- No individual microstructure can be used to diagnose environments in which the rock has been deformed. Even when analyzing sets of structures, micromorphology would not be the best method of determination. However, two distinct characteristics were observed in the studied deposits: the lines defined from a mass movement tend to be much more horizontal than those outlined in glaciotectionized deposits. There is also a greater presence of normal faults in MTDs than in glaciotectionites, corresponding to the most proximal part of the deposit.

2.7 References

- Allen, J.R.L.** (1982) *Sedimentary Structures: Their Character and Physical Basis*. Elsevier, Amsterdam.
- Almeida, F. F. M. and Hasui, Y.** (1984) *O Pré-Cambriano do Brasil*. Edgard Blücher, São Paulo, 378 p.
- Alsop, G.I. and Marco, S.** (2011) Soft-sediment deformation within seismogenic slumps of the Dead Sea Basin. *J. Struct. Geol.*, 33, 433–457.
- Alsop, G.I. and Marco, S.** (2013) Seismogenic slump folds formed by gravity-driven tectonics down a negligible subaqueous slope. *Tectonophysics*, 605, 48–69.
- Alsop, G.I., Marco, S., Levi, T. and Weinberger, R.** (2017) Fold and thrust systems in Mass Transport Deposits. *J. Struct. Geol.*, 94, 98–115
- Baroni, C. and Fasano, F.,** (2006). Micromorphological evidence of warm-based glacier deposition from the Ricker hills tillite (victoria land, Antarctica). *Quat. Sci. Rev.* 25, 976-992
- Busfield, M.E. and Le Heron, D.P.** (2013) Glacitectonic deformation in the chuos formation of northern namibia: Implications for neoproterozoic ice dynamics. *Proc. Geol. Assoc.*, 124, 778–789.
- Carr, S.J.** (2001) Micromorphological criteria for discriminating subglacial and glacialmarine sediments: evidence from a contemporary tidewater glacier, Spitsbergen. *Quatern. Int.*, **86**, 71–79.
- Carr, S.J. and Goddard, M.** (2007) Role of particle-size in the development of till fabric: implications for using eigenvectors in understanding glacier dynamics. *Boreas*. **36**, 371-385.
- Carr, S.J., Haflidason, H., and Sejrup, H.P.** (2000) Micromorphological evidence supporting late Weichselian glaciation of the Northern North Sea. *Boreas*, **29**, 315–328.
- Carr, S. J., Holmes, R., van der Meer, J. J. M. and Rose, J.** (2006) The Last Glacial Maximum in the North Sea Basin: micromorphological evidence of extensive glaciation. *J. Quat. Sci*, **21**, 131–153.
- Carr, S.J. and Rose, J.** (2003) Till fabric patterns and significance: particle response to subglacial stress. *Quaternary Science Reviews*, **22**, 1415 -1426.

- Collinson J.** (1994) Sedimentary deformational structures. In: *The Geological Deformation of Sediments* (Ed. A Maltman), pp 95-125. Springer, Dordrecht.
- Elliot, C.G. and Williams, P.F., 1988.** Sediment slump structures: a review of diagnostic criteria and application to an example from Newfoundland. *J. Struct. Geol.*, **10**, 171-182.
- Farrell, S. and Eaton, S.** (1988) Foliations developed during slump deformation of Miocene marine sediments, Cyprus. *J. Struct. Geol.*, **10**, 567–576.
- Fossen, H.** (2010). *Structural Geology*. Cambridge University Press, 524 p.
- França, A. B. and Potter, P. E.** (1988) Estratigrafia, ambiente deposicional e análise de reservatório do Grupo Itararé (Permocarbonífero), Bacia do Paraná (Part 1). *Boletim de Geociências da Petrobras*, Rio de Janeiro, **2(2-4)**, 147-191.
- Gesicki, A. L. D.** (1996) Geologia da Formação Aquidauana (Neopaleozoico, Bacia do Paraná) na porção centro-norte do estado de Mato Grosso do Sul. Dissertação de Mestrado. IGC, Universidade de São Paulo, São Paulo. 162 p.
- Gesicki, A. L. D., Riccomini, C., Boggiani, P. C., and Coimbra, A. M.** (1998) The Aquidauana Formation (Parana Basin) in the context of late Palaeozoic glaciation in western Gondwana. *Journal of African Earth Sciences*, **27(1)**, 81-82.
- Hiemstra, J.F., and van der Meer, J.J.M.** (1997) Pore-water controlled grain fracturing as an indicator for subglacial shearing in tills. *Journal of Glaciology* **43**, 446 - 454.
- Isbell, J.L., Miller, M.F., Wolfe, K.L. and Lenaker, P.A.** (2003) Timing of late Paleozoic glaciation in Gondwana: Was glaciation responsible for the development of northern hemisphere cyclothems? *Spec. Pap. Geol. Soc. Am.*, **370**, 5–24.
- Kilfeather, A. A., Ó Cofaigh, C., Dowdeswell, J. A., van der Meer, J. J. M. and Evans, D. J. A.** (2010) Micromorphological characteristics of glacialmarine sediments: implications for distinguishing genetic processes of massive diamicts. *Geo-Marine Letters*, **30**, 77–97.
- Lachniet, M.S., Larson, G.J., Lawson, D.E., Evenson, E.B., Alley, R.B.** (2001) Microstructures of sediment flow deposits and subglacial sediments: a comparison. *Boreas*, **30**, 254–262.
- Lachniet, M.S., Larson, G.J., Strasser, J.C., Lawson, D.E., Evenson, E.B.** (1999) Microstructures of glacial sediment flow deposits, Matanuska Glacier, Alaska. In: *Glacial Processes Past and Present* (Eds. Mickleson, D.M. and Attig, J.W). *Geological Society of America, Special Papers*, **337**, 45-57.
- Maltman, A. J.** (1981) Primary bedding-parallel fabrics in Structural Geology. *J. geol. Soc. Lond.*, **138**, 475—483.
- Maltman, A. J.** (1994) *The Geological Deformation of Sediments*. Springer, Dordrecht. 368p
- Menzies, J., van der Meer, J.J.M., and Rose, J.** (2006) Tills—as a glacial “tectomict,” its internal architecture and the development of a “typing” method for till differentiation. *Geomorphology*, **75**, 172–200.

- Menzies, J., van der Meer, J.J.M., and Ravier, E.** (2016) A kinematic unifying theory of microstructures in subglacial tills. *Sed. Geology*, **244**, 57-70p
- Menzies, J., Zaniewski, K., and Dreger, D.** (1997) Evidence from microstructures of deformable bed conditions within drumlins, Chimney Bluffs, New York State. *Sediment. Geol.*, **111**, 161–176.
- Milani, E. J.** (2004) Comentários sobre a origem e evolução tectônica da Bacia do Paraná. In: Geologia do Continente Sul-Americano: Evolução da Obra de Fernando Flávio Marques de Almeida (Eds. Mantesso-Neto, V., Bartorelli, A., Carneiro, C.D.R., and Brito-Neves, B.B.), pp.265-279. Beca, São Paulo.
- Moretti, M.**, 2000. Soft-sediment deformation structures interpreted as seismites in middle-late Pleistocene aeolian deposits (Apulian foreland, southern Italy). *Sedimentary Geology*, **135**, 167–179.
- Ogata, K., Mountjoy, J.J., Pini, G.A., Festa, A. and Tinterri, R.** (2014) Shear zone liquefaction in mass transport deposit emplacement: A multi-scale integration of seismic reflection and outcrop data. *Mar. Geol.*, **356**, 50–64.
- Owen, G.** (1987) Deformation processes in unconsolidated sands. In: Deformation of Sediments and Sedimentary Rocks (Eds. M.E. Jones, R.M.F. Preston), *Geological Society of London, Special Publications*, **29**, 11 – 24.
- Owen, G., Moretti, M. and Alfaro, P.** (2011) Recognising triggers for soft-sediment deformation: Current understanding and future directions. *Sediment. Geol.*, **235**, 133–140.
- Phillips, E. R.** (2006) Micromorphology of a debris flow deposit: evidence of basal shearing, hydrofracturing, liquefaction and rotational deformation during emplacement. *Quat. Sci. Rev.*, **25**, 720–738.
- Phillips, E., van der Meer, J.J.M. and Ferguson, A.** (2011) A new “microstructural mapping” methodology for the identification, analysis and interpretation of polyphase deformation within subglacial sediments. *Quat. Sci. Rev.*, **30**, 2570–2596.
- Phillips, E. R., Evans, D. J. A, van der Meer, J. J. M and Lee, J. R.** (2018). Microscale evidence of liquefaction and its potential triggers during soft-bed deformation within subglacial traction tills. *Quat. Sci. Rev.*, **181**(i), 123-143
- Reinardy, B.T.I. and Lukas, S.** (2009) The sedimentary signature of ice-contact sedimentation and deformation at macro- and microscale: a case study from NW Scotland. *Sediment. Geol.*, **221**, 87–98.
- Rodrigues, M.C.N.L, Trzaskos, B., Alsop, G.I. and Vesely, F.F.** (2020) Making a homogenite: An outcrop perspective into the evolution of deformation within mass-transport deposits. *Mar. Pet. Geol.*, **112**, 104033.
- Rosa, E.L.M., Vesely, F.F., Isbell, J.L., Kipper, F., Fedorchuk, N.D. and Souza, P.A.** (2019) Constraining the timing, kinematics and cyclicity of Mississippian-Early Pennsylvanian glaciations in the Paraná Basin, Brazil. *Sediment. Geol.*, **384**, 29–49.
- Shanmugam, G.** (2016) The seismite problem. *J. Palaeogeogr.*, **5**, 318–362.

Shanmugam, G. and Wang, Y. (2015) The landslide problem. *J. Palaeogeogr.*, 4, 109–166.

Sobiesiak, M.S., Kneller, B., Alsop, G.I. and Milana, J.P. (2016) Internal deformation and kinematic indicators within a tripartite mass transport deposit, NW Argentina. *Sediment. Geol.*, 344, 364–381.

van der Meer, J.J.M. (1987) Micromorphology of glacial sediments as a tool in distinguishing genetic varieties of till. In: INQUA Till Symposium 1987 (Eds. Kujansuu, R. and Saarnisto, M.). Geological Survey of Finland, vol. 3, pp. 77–89.

van der Meer, J. J.M. (1993) Microscopic evidence of subglacial deformation. *Quat. Sci. Rev.*, 12, 553–587.

van Der Meer, J.J.M., Menzies, J. and Rose, J. (2003) Subglacial till: The deforming glacier bed. *Quat. Sci. Rev.*, 22, 1659–1685.

van Der Meer, J.J.M., Menzies, J. (2011) The micromorphology of unconsolidated sediments. *Sed. Geology*, 238(3-4), 213-232

Vesely, F.F., Trzaskos, B., Kipper, F., Assine, M.L. and Souza, P.A. (2015) Sedimentary record of a fluctuating ice margin from the Pennsylvanian of western Gondwana: Paraná Basin, southern Brazil. *Sediment. Geol.*, 326, 45–63.

Vesely, F.F. and Assine, M.L. (2004) Sequências e tratos de sistemas deposicionais do Grupo Itararé, norte do Estado do Paraná. *Rev. Bras. Geociências*, 34, 219–230.

3. CONSIDERAÇÕES FINAIS

A análise em multiescala da deformação em sedimentos gerada por glacioteconismo e movimentos em massa das rochas depositadas durante a *Late Paleozoic Ice Age* na Bacia do Paraná a partir de dados estruturais de campo e dados obtidos a partir de técnicas para análise microscópica tradicionalmente utilizadas em depósitos recentes mostrou-se eficiente, sendo possível reconhecer mais de 20 microestruturas distintas e aplicar o método de mapeamento proposto por Phillips *et al.* 2011. Apesar disso, a diagênese mais intensa em rochas com pouca ou nenhuma matriz mas com que seja impossível reconhecer microestruturas nestas condições.

A amostragem para este trabalho teve um número consideravelmente maior de rochas glacioteconizadas em relação a movimentos de massa, desta forma estudos futuros com mais amostras provenientes de movimentos gravitacionais é incentivado.

Recomenda-se ainda a utilização de técnicas complementares para maior investigação da origem e desenvolvimento das micas que compõem as *plasmic fabrics*, tal como microsonda eletrônica e datações Ar/Ar. Assim como imageamento por microscópio eletrônico de varredura (MEV) e catodoluminescência para melhor caracterização de fases e feições diagenéticas.

REFERÊNCIAS

- Almeida, F. F. M. (1954). Geologia do centro-leste mato-grossense. Ministério da Agricultura, Departamento Nacional da Produção Mineral, Divisão de Geologia e Mineralogia.
- Allen, J.R.L. (1982) Sedimentary Structures: Their Character and Physical Basis. Elsevier, Amsterdam.
- Alsop, G.I. and Marco, S. (2011) Soft-sediment deformation within seismogenic slumps of the Dead Sea Basin. *J. Struct. Geol.*, 33, 433–457.
- Alsop, G.I. and Marco, S. (2013) Seismogenic slump folds formed by gravity-driven tectonics down a negligible subaqueous slope. *Tectonophysics*, 605, 48–69.
- Alsop, G.I., Marco, S., Levi, T. and Weinberger, R. (2017) Fold and thrust systems in Mass Transport Deposits. *J. Struct. Geol.*, 94, 98–115.
- Benn, D.I. and Prave, A.R. (2006) Subglacial and proglacial glacetectonic deformation in the Neoproterozoic Port Askaig Formation, Scotland. *Geomorphology*, 75, 266–280.
- Beurlen, K. (1956) A geologia pós-algonquiana do Estado de Mato Grosso. *DNPM/DGM, Notas Preliminares e Estudos, Bol*, 163, 7-187.
- Bordonau, J., van der Meer, J.J.M. (1994) An example of a kinking microfabric in Upper-Pleistocene glaciolacustrine deposits from Llavorsi (Central Southern Pyrenees, Spain). *Geol. Mijnb.* 73, 23-30.
- Busfield, M.E. and Le Heron, D.P. (2013) Glacetectonic deformation in the chuos formation of northern namibia: Implications for neoproterozoic ice dynamics. *Proc. Geol. Assoc.*, 124, 778–789.
- Busfield, M. E., and Le Heron, D. P. (2018). Snowball Earth under the microscope. *Journal of Sedimentary Research*, 88(5), 659-677.
- Canuto, J. R. (1993) Fácies e ambientes de sedimentação da Formação Rio do Sul (Permiano), Bacia do Paraná, na região de Rio do Sul, estado de Santa Catarina. Tese (Doutorado), Universidade de São Paulo, São Paulo. 164 p.
- Carr, S. (2004) Micro-scale features and structures. In: A Practical Guide to the Study of Glacial Sediments (Eds. Evans, D.J.A., Benn, D.I.), pp. 115–144. Hodder Arnold, London.
- Caster, K. E. (1947) Expedição geológica em Goiás e Mato Grosso. *Mineração e Metalurgia*, 12(69), 126-127.
- Collinson J. (1994) Sedimentary deformational structures. In: The Geological Deformation of Sediments (Ed. A Maltman), pp 95-125. Springer, Dordrecht.

Darvill, C.M., Stokes, C.R., Bentley, M.J., Evans, D.J.A. and Lovell, H. (2017) Dynamics of former ice lobes of the southernmost Patagonian Ice Sheet based on a glacial landsystems approach. *J. Quat. Sci.*, 32, 857–876.

Eyles, C.H. and Eyles, N. (2000) Subaqueous mass flow origin for Lower Permian diamictites and associated facies of the Grant Group, Barwire Terrace, Canning Basin, Western Australia. *Sedimentology*, 47, 343–356.

Eyles C.H., Eyles N., França A.B. (1993) Glaciation and tectonics in an active intracratonic basin: the Late Palaeozoic Itararé Group, Paraná Basin, Brazil. *Sedimentology*, 40(1), 1-25.

Farjallat, J. E. S. (1970) Diamictitos neopaleozóicos e sedimentos associados do sul de Mato Grosso. Tese de Doutorado. Universidade de São Paulo, São Paulo, 66 p.

Fedorchuk, N.D., Isbell, J.L., Griffis, N.P., Vesely, F.F., Rosa, E.L.M., Montáñez, I.P., Mundil, R., Yin, Q.Z., Iannuzzi, R., Roesler, G. and Pauls, K.N. (2019) Carboniferous glaciotectionized sediments in the southernmost Paraná Basin, Brazil: Ice marginal dynamics and paleoclimate indicators. *Sediment. Geol.*, 389, 54–72.

França, A. B., Potter, P. E. (1988) Estratigrafia, ambiente deposicional e análise de reservatório do Grupo Itararé (Permocarbonífero), Bacia do Paraná (Parte 1). *Boletim de Geociências da Petrobras*, Rio de Janeiro, 2(2-4), 147-191.

Gama Jr, E. G., Perinotto, J. A., Ribeiro, H. J., and Padula, E. K. (1992) Contribuição ao estudo da ressedimentação no Subgrupo Itararé: tratos de fácies e hidrodinâmica deposicional. *Revista Brasileira de Geociências*, 22(2), 228-236.

Gesicki, A. L. D. (1996) Geologia da Formação Aquidauana (Neopaleozoico, Bacia do Paraná) na porção centro-norte do estado de Mato Grosso do Sul. Dissertação de Mestrado. IGC, Universidade de São Paulo, São Paulo. 162 p.

Gesicki, A. L. D., Riccomini, C., and Boggiani, P. C. (2002). Ice flow direction during late Paleozoic glaciation in western Paraná Basin, Brazil. *Journal of South American Earth Sciences*, 14(8), 933-939.

Gesicki, A. L. D., Riccomini, C., Boggiani, P. C., and Coimbra, A. M. (1998) The Aquidauana Formation (Parana Basin) in the context of late Palaeozoic glaciation in western Gondwana. *Journal of African Earth Sciences*, 27(1), 81-82.

Guirro, A. C. (1991). Análise de fácies dos sedimentos da Formação Aquidauana (Neocarbonífero) no sudeste de Mato Grosso e nos poços da borda norte da Bacia do Paraná. Dissertação de Mestrado. Departamento de Geologia, Universidade Federal de Ouro Preto, Ouro Preto. 184 p.

Isbell, J.L., Miller, M.F., Wolfe, K.L. and Lenaker, P.A. (2003) Timing of late Paleozoic glaciation in Gondwana: Was glaciation responsible for the development of northern hemisphere cyclothems? *Spec. Pap. Geol. Soc. Am.*, 370, 5–24.

- Le Heron, D.P., Sutcliffe, O.E., Whittington, R.J. and Craig, J. (2005) The origins of glacially related soft-sediment deformation structures in Upper Ordovician glaciogenic rocks: Implication for ice-sheet dynamics. *Palaeogeogr. Palaeoclimatol. Palaeoecol.*, 218, 75–103.
- Maltman, A. (1994) *The Geological Deformation of Sediments*. Springer, Dordrecht. 368p.
- Martinsen, O.J. (1994) Mass movements. In: *The Geological Deformation of Sediments* (Ed. A Maltman), pp. 127-165. Springer, Dordrecht.
- Martinsen, O.J., Lien, T., Walker, R.G. and Collinson, J.D. (2003) Facies and sequential organisation of a mudstone-dominated slope and basin floor succession: The Gull Island Formation, Shannon Basin, Western Ireland. *Mar. Pet. Geol.*, 20, 789–807.
- Menzies, J. (1998). Microstructures within subglacial diamictites. Relief and deposits of present-day and pleistocene glaciations of the northern hemisphere—selected problems. *Geography Series*, 58, 210-216.
- Menzies, J. and van der Meer, J.J.M. (2017) *Micromorphology and Microsedimentology of Glacial Sediments*. Elsevier Ltd, 753-806 pp.
- Milani, E. J. (1997) Evolução tectono-estratigráfica da Bacia do Paraná e seu relacionamento com a geodinâmica fanerozóica do Gondwana sul-ocidental. Tese (Doutorado), Universidade Federal do Rio Grande do Sul, Porto Alegre, 2 v.
- Milani, E. J., Melo, J. H. G., Souza, P. A., Fernandes, L. A., França, A. B. (2007) Bacia do Paraná. *Boletim de Geociências da Petrobras*, Rio de Janeiro, 15(2), 265–287.
- Moretti, M., 2000. Soft-sediment deformation structures interpreted as seismites in middle-late Pleistocene aeolian deposits (Apulian foreland, southern Italy). *Sedimentary Geology*, 135, 167–179.
- Mottin, T.E., Vesely, F.F., de Lima Rodrigues, M.C.N., Kipper, F. and de Souza, P.A. (2018) The paths and timing of late Paleozoic ice revisited: New stratigraphic and paleo-ice flow interpretations from a glacial succession in the upper Itararé Group (Paraná Basin, Brazil). *Palaeogeogr. Palaeoclimatol. Palaeoecol.*, 490, 488–504.
- Ogata, K., Mountjoy, J.J., Pini, G.A., Festa, A. and Tinterri, R. (2014) Shear zone liquefaction in mass transport deposit emplacement: A multi-scale integration of seismic reflection and outcrop data. *Mar. Geol.*, 356, 50–64.
- Owen, G. (1987) Deformation processes in unconsolidated sands. In: *Deformation of Sediments and Sedimentary Rocks* (Eds. M.E. Jones, R.M.F. Preston), *Geological Society of London, Special Publications*, 29, 11 – 24.
- Owen, G., Moretti, M. and Alfaro, P. (2011) Recognising triggers for soft-sediment deformation: Current understanding and future directions. *Sediment. Geol.*, 235, 133–140.

Passchier, C. W., Trouw, R. A. J. (1996) *Microtectonics*. Springer-Verlag, Berlin. 289 p.

Petri, S., and Fúlfaro, V. J. (1966). Sobre a geologia da área balizada pelas cidades de Barra do Garças e Guiratinga, Mato Grosso e Jataí e Amorinópolis, Goiás. *Boletim Sociedade Brasileira de Geologia*, 15(3), 59-80.

Phillips, E. R. (2006) Micromorphology of a debris flow deposit: evidence of basal shearing, hydrofracturing, liquefaction and rotational deformation during emplacement. *Quat. Sci. Rev.*, 25, 720–738.

Phillips, E., van der Meer, J.J.M. and Ferguson, A. (2011) A new “microstructural mapping” methodology for the identification, analysis and interpretation of polyphase deformation within subglacial sediments. *Quat. Sci. Rev.*, 30, 2570–2596.

Posamentier, H. W., Martinsen, O. J., and Shipp, R. C. (2011). The character and genesis of submarine mass-transport deposits: insights from outcrop and 3D seismic data. *Mass-transport deposits in deepwater settings. SEPM, Special Publication*, 96, 7-38.

Posamentier, H. G., Walker, R. G. (2006) Facies Models Revisited, *SEPM Special Publication*, 84, 1-17.

Rocha-Campos, A.C. (1967) The Tubarão Group in the Brazilian portion of the Paraná Basin. In: *Problems in Brazilian Gondwana Geology*, 9 (Eds. Bigarella, J. J., Becker, R. R. Pinto, I. D.). Curitiba, IG-UFPR, 27-102.

Rocha-Campos, A. C., and Dos Santos, P. R. (1981) The Itararé subgroup, Aquidauana group and San Gregorio formation, Parana basin, southeastern south America. *Earth's pre-Pleistocene glacial record*, 842-852.

Rodrigues, M.C.N.L, Trzaskos, B., Alsop, G.I. and Vesely, F.F. (2020) Making a homogenite: An outcrop perspective into the evolution of deformation within mass-transport deposits. *Mar. Pet. Geol.*, 112, 104033.

Rosa, E.L.M., Vesely, F.F. and França, A.B. (2016) A review on late Paleozoic ice-related erosional landforms in the Paraná Basin: Origin and paleogeographical implications. *Brazilian J. Geol.*, 46, 147–166.

Rosa, E.L.M., Vesely, F.F., Isbell, J.L., Kipper, F., Fedorchuk, N.D. and Souza, P.A. (2019) Constraining the timing, kinematics and cyclicity of Mississippian-Early Pennsylvanian glaciations in the Paraná Basin, Brazil. *Sediment. Geol.*, 384, 29–49.

Schemiko, D.C.B., Vesely, F.F. and Rodrigues, M.C.N.L. (2019) Deepwater to fluvio-deltaic stratigraphic evolution of a deglaciated depocenter: The early Permian Rio do Sul and Rio Bonito formations, southern Brazil. *J. South Am. Earth Sci.*, 95, 102260.

- Schneider, R. L., Mühlmann, H., Tommasi, E., Medeiros, R. A., Daemon, R. F., Nogueira, A. A. (1974) Revisão estratigráfica da Bacia do Paraná. *Anais...Congresso Brasileiro de Geologia* n. 28, 1974, Porto Alegre. São Paulo: Sociedade Brasileira de Geologia, v. 1, 41-65.
- Shanmugam, G. (2016) The seismite problem. *J. Palaeogeogr.*, 5, 318–362.
- Shanmugam, G. and Wang, Y. (2015) The landslide problem. *J. Palaeogeogr.*, 4, 109–166.
- Sitler, R. F., Chapman, C. A. (1955) Microfabrics of tills. *Journal of Sedimentary Petrology*, 25(4), 262-269.
- Sitler, R. F. (1968) Glacial till in oriented thin sections. *Proc... XXIII International Geological Congress*, vol. 8, 283-295.
- Sobiesiak, M.S., Kneller, B., Alsop, G.I. and Milana, J.P. (2016) Internal deformation and kinematic indicators within a tripartite mass transport deposit, NW Argentina. *Sediment. Geol.*, 344, 364–381.
- Suss, J.F., Vesely, F.F., Santa Catharina, A., Assine, M.L., Paim, P.S.G. (2014) O Grupo Itararé (Neocarbonífero-eopermiano) entre Porto Amazonas (PR) e Mafra (SC): Sedimentação gravitacional em contexto marinho deltaico com influência glacial. *Geociências*, 33, 701–719.
- Vail, P. R., Mitchum, R. M., Thompson, S. (1977) Seismic stratigraphy and global changes of sea level, part 3: relative changes of sea level from coastal onlap. In: *Seismic stratigraphy: applications to hydrocarbon exploration* (Ed. C. E. Payton). American Association of Petroleum Geologists, *Memoir*, 26, 63-81.
- van der Meer, J.J.M. (1987) Micromorphology of glacial sediments as a tool in distinguishing genetic varieties of till. *Geological Survey of Finland, Special Paper*, 3, 77-89.
- van der Meer, J.J.M. (1993) Microscopic evidence of subglacial deformation. *Quat. Sci. Rev.*, 12, 553–587.
- van der Meer, J.J.M. (1996) Micromorphology. In: *Glacial environments*, vol. 2 (Ed. J Menzies), pp. 335–355. Butterworth & Heinemann, Oxford.
- van Der Meer, J.J.M., Menzies, J. and Rose, J. (2003) Subglacial till: The deforming glacier bed. *Quat. Sci. Rev.*, 22, 1659–1685.
- van Der Meer, J.J.M., Menzies, J. (2011) The micromorphology of unconsolidated sediments. *Sed. Geology*, 238(3-4), 213-232
- Vesely, F.F., Trzaskos, B., Kipper, F., Assine, M.L. and Souza, P.A. (2015) Sedimentary record of a fluctuating ice margin from the Pennsylvanian of western Gondwana: Paraná Basin, southern Brazil. *Sediment. Geol.*, 326, 45–63.
- Zaniewski, K. (2001) Plasmic fabric analysis of glacial sediments using quantitative image analysis methods and GIS techniques. Universiteit van Amsterdam.